

# Local discontinuous Galerkin methods with implicit-explicit time-marching for multi-dimensional convection-diffusion problems

Haijin Wang<sup>†</sup>   Shiping Wang<sup>‡</sup>   Qiang Zhang<sup>†</sup>   Chi-Wang Shu<sup>§</sup>

August 28, 2015

## Abstract

The main purpose of this paper is to analyze the stability and error estimates of the local discontinuous Galerkin (LDG) methods coupled with implicit-explicit (IMEX) time discretization schemes, for solving multi-dimensional convection-diffusion equations with nonlinear convection. By establishing the important relationship between the gradient and the interface jump of the numerical solution with the independent numerical solution of the gradient in the LDG method, on both rectangular and triangular elements, we can obtain the same stability results as in the one-dimensional case [14, 15], i.e, the IMEX LDG schemes are unconditionally stable for the multi-dimensional convection-diffusion problems, in the sense that the time-step  $\tau$  is only required to be upper-bounded by a positive constant independent of the spatial mesh size  $h$ . Furthermore, by the aid of the so-called elliptic projection and the adjoint argument, we can also obtain optimal error estimates in both space and time, for the corresponding fully discrete IMEX LDG schemes, under the same condition, i.e, if piecewise polynomial of degree  $k$  is adopted on either rectangular or triangular meshes, we can show the convergence accuracy is of order  $\mathcal{O}(h^{k+1} + \tau^s)$  for the  $s$ -th order IMEX LDG scheme ( $s = 1, 2, 3$ ) under consideration. Numerical experiments are also given to verify our main results.

**keywords.** local discontinuous Galerkin method, implicit-explicit scheme, convection-diffusion, stability, error estimate.

**AMS.** 65M12, 65M15, 65M60

## 1 Introduction

In this paper we carry out the stability analysis and error estimates of a fully discrete local discontinuous Galerkin (LDG) scheme coupled with implicit-explicit Runge-Kutta time

---

<sup>†</sup>Department of Mathematics, Nanjing University, Nanjing 210093, Jiangsu Province, P. R. China. E-mail: hjwang@smail.nju.edu.cn; qzh@nju.edu.cn. Research supported by NSFC grant 11271187.

<sup>‡</sup>College of Shipbuilding Engineering, Harbin Engineering University, Harbin 15000, P. R. China. E-mail: wangshiping@hrbeu.edu.cn. Research supported by NSFC grant 11202057.

<sup>§</sup>Division of Applied Mathematics, Brown University, Providence, RI 02912, U.S.A. E-mail: shu@dam.brown.edu. Research supported by DOE grant DE-FG02-08ER25863 and NSF grant DMS-1418750.

discretization, for solving nonlinear multi-dimensional scalar convection-diffusion problems

$$U_t + \nabla \cdot \mathbf{F}(U) = \Delta U, \quad (\mathbf{x}, t) \in Q_T = \Omega \times (0, T], \quad (1.1)$$

with periodic boundary condition and the initial solution  $U(\mathbf{x}, 0) = U_0(\mathbf{x})$ . Here  $\Omega$  is a bounded rectangular domain in  $\mathbb{R}^d$  ( $d = 2, 3$ ), and  $\mathbf{F}(U) = (f_1(U), \dots, f_d(U))$  is the given flux function whose components are assumed to be smooth enough.

The LDG method was introduced by Cockburn and Shu for convection-diffusion problems in [7], motivated by the work of Bassi and Rebay [2] for compressible Navier-Stokes equations. As an extension of discontinuous Galerkin (DG) schemes for hyperbolic conservation laws [8], this scheme shares the advantages of the DG methods, such as good stability, high order accuracy, and flexibility on  $h$ - $p$  adaptivity and on complex geometry. Besides, a key advantage of this scheme is the local solvability, that is, the auxiliary variables approximating the gradient of the solution can be locally eliminated. The LDG schemes have also been successfully designed for other diffusion problems, for example, the bi-harmonic equations [23, 9], the Kuramoto-Sivashinsky type equations [20], the Cahn-Hilliard equation [19], etc. Moreover, the LDG schemes have been studied for solving dispersive equations as well, such as KdV-type equations [22], the fifth order convection dispersion equation [23], etc. For more applications of the LDG schemes, we refer the readers to the review article [21] and the reference therein.

The LDG scheme has shown its good stability for many types of problems [21] in the semi-discrete framework. However, efficient time discretization is an important issue to be studied, especially for high order spatial derivative problems. As for convection-diffusion problems, explicit Runge-Kutta time discretization methods analyzed in [16] is stable, efficient and accurate for solving convection-dominated convection-diffusion problems. However, for convection-diffusion equations which are not convection-dominated, explicit time discretization will suffer from a stringent time step restriction for stability [18]. When it comes to such problems, a natural consideration to overcome the small time step restriction is to use implicit time marching. Furthermore, in many applications the convection terms are often nonlinear, hence it would be desirable to treat them explicitly while using implicit time discretization only for the linear diffusion terms. Such time discretizations are called implicit-explicit (IMEX) time discretizations [1]. Even for nonlinear diffusion terms, IMEX time discretizations would show their advantages in obtaining an elliptic algebraic system, which is easy to solve by many iterative methods. If both convection and diffusion are treated implicitly, the resulting algebraic system will be far from elliptic and convergence of many iterative solvers will suffer.

In [14, 15], we showed that the three specific Runge-Kutta type IMEX schemes given in [1] and [3], coupled with LDG spatial discretization for solving one-dimensional linear and nonlinear convection-diffusion problems, are unconditional stable in the sense that the time step  $\tau$  is only required to be upper bounded by a constant which is independent of the mesh size  $h$ . In this paper, we will show that the same stability holds for the IMEX LDG schemes considered in [14] for solving multi-dimensional nonlinear convection-diffusion problems, on both rectangular meshes and triangular meshes. We would like to point out that, for rectangular meshes, we consider the finite element space as piecewise polynomials of degree  $k$ , denoted as  $\mathcal{P}_k$ , just as for the triangular case. This is different from the traditional treatment in the literatures, such as [6, 9], where finite element spaces

with tensor product polynomials were considered. Furthermore, it is worth mentioning that, our stability analysis on multi-dimensional space also relies heavily on the important relationship between the auxiliary variable and the primal variable, which is formally the same as the one-dimension case, however, the proof is not straightforward for  $\mathcal{P}_k$  elements, especially for the triangular meshes.

In this paper, we also perform the error estimates for the IMEX LDG methods. Unlike the one-dimensional case, in multi-dimensional case, we cannot find a proper projection to eliminate the element boundary errors to obtain the optimal error estimate. To get an optimal error estimate, we would like to utilize the so called *elliptic projection* which is a standard tool in the numerical analysis for elliptic and parabolic problems [17, 13]. This method was also used in [9] to derive the optimal error estimate for the LDG method solving linear time-dependent fourth order problems on triangular elements. In this paper, we will follow [9] and adopt this methodology to derive the optimal error estimate for the IMEX LDG methods on both rectangular and triangular meshes. We will obtain  $(k + 1)$ -th order of accuracy if the finite element space is made up of piecewise polynomials of degree  $k$ .

The paper is organized as follows. In Section 2 we present the semi-discrete as well as the fully-discrete LDG schemes for the model problem. In Section 3 we give some preliminaries, including some basic inequalities, the key lemma and the useful elliptic projection. Sections 4, 5 are devoted to the stability and error analysis for the IMEX LDG methods. In Section 6 we will present some numerical results to verify our results. The concluding remarks and some technical proofs are given in Section 7 and the Appendix, respectively.

## 2 The LDG method with IMEX time-marching

In this section we will present the definition of the LDG scheme with IMEX time-marching, for problem (1.1). For simplicity, we only consider the two dimensional case ( $d = 2$ ) in this paper, in which  $\mathbf{x} = (x, y)$  and  $\mathbf{F}(U) = (f(U), g(U))$ . The results can be easily extended to the three dimensional case ( $d = 3$ ).

### 2.1 Discontinuous finite element space

Let  $\Omega_h = \{K\}$  be a quasi-uniform partition of the domain  $\Omega$  with triangular (or rectangular) element  $K$ , where  $h = \max_K h_K$ , with  $h_K$  being the diameter of element  $K$ . We denote  $\Gamma_h$  as the set of all element interfaces. Associated with this mesh, we define the discontinuous finite element space

$$V_h = \{ v \in L^2(\Omega) : v|_K \in \mathcal{P}_k(K), \forall K \in \Omega_h \}, \quad (2.1)$$

where  $\mathcal{P}_k(K)$  denotes the space of polynomials of degree less than or equal to  $k$  in  $K$ .

Following [22, 21], we choose a fixed vector  $\boldsymbol{\beta}$  which is not parallel with any normals of element boundaries. This is possible because there are only finitely many element boundary normals for any given mesh. For each side  $e$ , we use this fixed vector  $\boldsymbol{\beta}$  to uniquely define the *left* and *right* elements  $K_L$  and  $K_R$  which share the same side  $e$ . Namely,  $\boldsymbol{\beta} \cdot \mathbf{n}_{K_L} > 0$  and  $\boldsymbol{\beta} \cdot \mathbf{n}_{K_R} < 0$ , respectively, where  $\mathbf{n}_K$  is the outward normal of  $K$ . Along the side  $e$ , there are two traces for any function  $p$ , denoted by  $p^+ = (p|_{K_R})|_e$  and  $p^- = (p|_{K_L})|_e$ , respectively, and we denote the *jump* as  $\llbracket p \rrbracket = p^+ - p^-$ .

## 2.2 The semi-discrete LDG scheme

The semi-discrete LDG scheme [7, 21] starts from the following equivalent first-order differential system

$$U_t + \nabla \cdot (\mathbf{F}(U) - \mathbf{Q}) = 0, \quad \mathbf{Q} - \nabla U = 0, \quad (\mathbf{x}, t) \in Q_T, \quad (2.2)$$

with the same initial condition and boundary condition, where

$$\mathbf{Q} = (Q_1, Q_2) = (U_x, U_y) = \nabla U. \quad (2.3)$$

We would like to find the numerical solution of the LDG scheme, denoted by  $(u, \mathbf{q})$ , in the finite element space  $V_h \times \mathbf{V}_h$ , where  $\mathbf{V}_h = V_h^d$ .

Take the initial condition  $u(\mathbf{x}, 0) \in V_h$  as any approximation of the given initial solution  $U_0(\mathbf{x})$ . For any  $t > 0$ , the numerical solution  $(u(\mathbf{x}, t), \mathbf{q}(\mathbf{x}, t)) \in V_h \times \mathbf{V}_h$  satisfies the variation forms (in what follows we omit  $\mathbf{x}$  and  $t$  if there is no confusion)

$$(u_t, v)_K = \mathcal{H}_K(u, v) + \mathcal{L}_K(\mathbf{q}, v), \quad (2.4a)$$

$$(\mathbf{q}, \mathbf{r})_K = \mathcal{Q}_K(u, \mathbf{r}) \quad (2.4b)$$

in each element  $K$ , for any test functions  $(v, \mathbf{r}) \in V_h \times \mathbf{V}_h$ . Here

$$\mathcal{H}_K(u, v) = (\mathbf{F}(u), \nabla v)_K - \langle \tilde{F}_{\mathbf{n}_K, K}(u^{int_K}, u^{ext_K}), v \rangle_{\partial K}, \quad (2.5a)$$

$$\mathcal{L}_K(\mathbf{q}, v) = -(\mathbf{q}, \nabla v)_K + \langle \tilde{\mathbf{q}} \cdot \mathbf{n}_K, v \rangle_{\partial K}, \quad (2.5b)$$

$$\mathcal{Q}_K(u, \mathbf{r}) = -(u, \nabla \cdot \mathbf{r})_K + \langle \tilde{u}, \mathbf{r} \cdot \mathbf{n}_K \rangle_{\partial K}, \quad (2.5c)$$

where  $\mathbf{n}_K$  is the outward normal vector of each edge of element  $K$ ,  $u^{int_K}$  and  $u^{ext_K}$  denote the values of  $u$  evaluated from inside and outside from the element  $K$ , respectively. Also

$$(u, v)_K = \int_K uv \, dx dy, \quad (\mathbf{q}, \mathbf{r})_K = \int_K \mathbf{q} \cdot \mathbf{r} \, dx dy, \quad \text{and} \quad \langle u, v \rangle_{\partial K} = \int_{\partial K} uv \, ds \quad (2.6)$$

are the standard inner products in  $L^2(K)$  and  $L^2(\partial K)$ , respectively.

In (2.5), the ‘‘tilde’’ terms represent the numerical flux.  $\tilde{F}_{\mathbf{n}_K, K}(u^{int_K}, u^{ext_K})$  is any one-dimensional locally Lipschitz flux which is conservative and consistent with  $\mathbf{F}(u) \cdot \mathbf{n}_K$ . Namely,  $\tilde{F}_{\mathbf{n}_K, K}(u, u) = \mathbf{F}(u) \cdot \mathbf{n}_K$ , and  $\tilde{F}_{\mathbf{n}_K, K}(a, b) + \tilde{F}_{\mathbf{n}_{K'}, K'}(b, a) = 0$  for arbitrary  $a, b$ , where  $K$  and  $K'$  share the same edge; see [22] for more details. There are several well-known numerical fluxes which can be used, such as the Godunov flux, the Lax-Friedrichs flux, the Engquist-Osher flux, and so on. In addition, we adopt the alternating numerical flux [7] for  $\tilde{\mathbf{q}}$  and  $\tilde{u}$  in (2.5b) and (2.5c), for example,

$$\tilde{\mathbf{q}} = \mathbf{q}^+, \quad \tilde{u} = u^-. \quad (2.7)$$

We have now defined the semi-discrete LDG scheme.

For the convenience of analysis, we would like to write the above semi-discrete LDG scheme into the global form. By summing up the variational formulations (2.4) over all elements, we arrive at the compact form:

$$(u_t, v)_{\Omega_h} = \mathcal{H}(u, v) + \mathcal{L}(\mathbf{q}, v), \quad (2.8a)$$

$$(\mathbf{q}, \mathbf{r})_{\Omega_h} = \mathcal{Q}(u, \mathbf{r}), \quad (2.8b)$$

where  $(\cdot, \cdot)_{\Omega_h} = \sum_K (\cdot, \cdot)_K$  is the standard inner product in  $L^2(\Omega_h)$ . Here

$$\mathcal{H}(\cdot, \cdot) = \sum_K \mathcal{H}_K(\cdot, \cdot), \quad (2.9)$$

and similarly for  $\mathcal{L}$  and  $\mathcal{Q}$ .

### 2.3 The fully discrete LDG schemes

In this subsection we would like to present the fully-discrete LDG schemes coupled with three specific IMEX Runge-Kutta time-marching methods up to the third order, which have been considered in [14, 15] for one-dimensional convection-diffusion equations.

Let  $\{t^n = n\tau\}_{n=0}^M$  be the uniform partition of the time interval  $[0, T]$ , with time step  $\tau$  such that  $M\tau = T$ . The time step could actually change from step to step, but in this paper we take the time step as a constant for simplicity. Given  $u^n$ , hence  $(u^n, \mathbf{q}^n)$ , we would like to find the numerical solution at the next time level  $t^{n+1}$ , maybe through several intermediate stages  $t^{n,\ell}$ , by the following IMEX RK methods.

The LDG scheme with the first order IMEX time-marching method, where the convection part is treated by the forward Euler method and the diffusion part is treated by the backward Euler method, is given in the following form:

$$(u^{n+1}, v)_{\Omega_h} = (u^n, v)_{\Omega_h} + \tau \mathcal{H}(u^n, v) + \tau \mathcal{L}(\mathbf{q}^{n+1}, v), \quad (2.10a)$$

$$(\mathbf{q}^{n+1}, \mathbf{r})_{\Omega_h} = \mathcal{Q}(u^{n+1}, \mathbf{r}), \quad (2.10b)$$

for any function  $(v, \mathbf{r}) \in V_h \times \mathbf{V}_h$ .

The LDG scheme with the second order IMEX time marching scheme given in [1] is:

$$(u^{n,1}, v)_{\Omega_h} = (u^n, v)_{\Omega_h} + \gamma \tau \mathcal{H}(u^n, v) + \gamma \tau \mathcal{L}(\mathbf{q}^{n,1}, v), \quad (2.11a)$$

$$(u^{n+1}, v)_{\Omega_h} = (u^n, v)_{\Omega_h} + \delta \tau \mathcal{H}(u^n, v) + (1 - \delta) \tau \mathcal{H}(u^{n,1}, v) \\ + (1 - \gamma) \tau \mathcal{L}(\mathbf{q}^{n,1}, v) + \gamma \tau \mathcal{L}(\mathbf{q}^{n+1}, v), \quad (2.11b)$$

$$(\mathbf{q}^{n,\ell}, \mathbf{r})_{\Omega_h} = \mathcal{Q}(u^{n,\ell}, \mathbf{r}), \quad \ell = 1, 2, \quad (2.11c)$$

for any function  $(v, \mathbf{r}) \in V_h \times \mathbf{V}_h$ , where  $\gamma = 1 - \frac{\sqrt{2}}{2}$  and  $\delta = 1 - \frac{1}{2\gamma}$ . Here  $u^{n,2} = u^{n+1}$  and  $\mathbf{q}^{n,2} = \mathbf{q}^{n+1}$ .

The LDG scheme with the third order IMEX time marching scheme proposed in [3] reads: for any function  $(v, \mathbf{r}) \in V_h \times \mathbf{V}_h$ ,

$$(u^{n,\ell}, v)_{\Omega_h} = (u^n, v)_{\Omega_h} + \tau \sum_{\kappa=0}^3 (a_{\ell\kappa} \mathcal{H}(u^{n,\kappa}, v) + \tilde{a}_{\ell\kappa} \mathcal{L}(\mathbf{q}^{n,\kappa}, v)), \quad \ell = 1, 2, 3, \quad (2.12a)$$

$$(u^{n+1}, v)_{\Omega_h} = (u^n, v)_{\Omega_h} + \tau \sum_{\kappa=0}^3 (b_{\kappa} \mathcal{H}(u^{n,\kappa}, v) + \tilde{b}_{\kappa} \mathcal{L}(\mathbf{q}^{n,\kappa}, v)), \quad (2.12b)$$

$$(\mathbf{q}^{n,\ell}, \mathbf{r})_{\Omega_h} = \mathcal{Q}(u^{n,\ell}, \mathbf{r}), \quad \ell = 1, 2, 3, \quad (2.12c)$$

where the coefficients are given in the following tabular

$a_{\ell\kappa}$	$\gamma$	0	0	0	0	$\gamma$	0	0	$\tilde{a}_{\ell\kappa}$
	$\frac{1+\gamma}{2} - \alpha_1$	$\alpha_1$	0	0	0	$\frac{1-\gamma}{2}$	$\gamma$	0	
	0	$1 - \alpha_2$	$\alpha_2$	0	0	$\theta_1$	$\theta_2$	$\gamma$	
$b_\kappa$	0	$\theta_1$	$\theta_2$	$\gamma$	0	$\theta_1$	$\theta_2$	$\gamma$	$\tilde{b}_\kappa$

(2.13)

The left half of the tabular lists  $a_{\ell\kappa}$  and  $b_\kappa$ , with the columns from left to right corresponding to  $\kappa = 0, 1, 2, 3$ , and the first three rows from top to bottom corresponding to  $\ell = 1, 2, 3$ . Similarly, the right half lists  $\tilde{a}_{\ell\kappa}$  and  $\tilde{b}_\kappa$ . Here  $\gamma \approx 0.435866521508459$ ,  $\theta_1 = -\frac{3}{2}\gamma^2 + 4\gamma - \frac{1}{4}$ ,  $\theta_2 = \frac{3}{2}\gamma^2 - 5\gamma + \frac{5}{4}$ ,  $\alpha_1 = -0.35$  as in [3] and  $\alpha_2 = \frac{\frac{1}{3}-2\gamma^2-2\theta_2\alpha_1\gamma}{\gamma(1-\gamma)}$ .

### 3 Preliminaries

#### 3.1 The trace inverse inequalities

Now we present the following trace inverse property with respect to the finite element space  $V_h$ . For any function  $v \in V_h$ , and  $\mathbf{r} \in \mathbf{V}_h$ , there exists a positive inverse constant  $\mu > 0$  independent of  $v, \mathbf{r}, h$  and  $K$  such that

$$\|v\|_{\partial K} \leq \sqrt{\mu h^{-1}} \|v\|_K, \quad \|\mathbf{r} \cdot \mathbf{n}_K\|_{\partial K} \leq \sqrt{\mu h^{-1}} \|\mathbf{r}\|_K. \quad (3.1)$$

In this paper, we use  $\|\cdot\|_D$  to denote the standard  $L^2$  norm on domain  $D$ , if  $D = \Omega$ , we omit the subscript  $\Omega$  for simplicity.

In the following analysis, we will also use the global form of the above trace inverse inequalities by summing up the above local forms over every element  $K$ . The conclusions are the same since the mesh is assumed to be quasi-uniform, and we omit them.

#### 3.2 The main lemma

In this subsection, we give the main lemma to illustrate an important relationship between the gradient and the element interface jump of the numerical solution with the numerical solution of the gradient, which plays a key role in the two-dimensional analysis.

**Lemma 3.1.** *Suppose  $(u, \mathbf{q}) \in V_h \times \mathbf{V}_h$  is the solution of scheme (2.8b), namely*

$$(\mathbf{q}, \mathbf{r})_{\Omega_h} = \mathcal{Q}(u, \mathbf{r}), \quad \forall \mathbf{r} \in \mathbf{V}_h, \quad (3.2)$$

*then there exists a positive constant  $C_\mu$  independent of  $h$  but maybe depending on the inverse constant  $\mu$ , such that*

$$\|\nabla u\| + \sqrt{\mu h^{-1}} \|\llbracket u \rrbracket\|_{\Gamma_h} \leq C_\mu \|\mathbf{q}\|. \quad (3.3)$$

Here  $\|\cdot\|_{\Gamma_h} = (\sum_{e \in \Gamma_h} \|\cdot\|_e^2)^{1/2}$ .

To prove this lemma, we just need to consider it in an element  $K$ . By (2.4b), (2.5c) and integrating by parts we obtain

$$\begin{aligned} (\mathbf{q}, \mathbf{r})_K &= (\nabla u, \mathbf{r})_K - \langle u, \mathbf{r} \cdot \mathbf{n}_K \rangle_{\partial K} + \langle \tilde{u}, \mathbf{r} \cdot \mathbf{n}_K \rangle_{\partial K} \\ &= (\nabla u, \mathbf{r})_K - \langle \llbracket u \rrbracket, \mathbf{r} \cdot \mathbf{n}_K \rangle_{\partial K^-}. \end{aligned} \quad (3.4)$$

Here we use  $\partial_K^- = \{e \in \partial K, \boldsymbol{\beta} \cdot \mathbf{n}_K|_e < 0\}$  to denote the *inflow* side(s) of element  $K$ , if  $\boldsymbol{\beta} \cdot \mathbf{n}_K|_e > 0$ , we call  $e$  an *outflow* side of element  $K$ , where  $\mathbf{n}_K|_e$  denotes the outward unit normal to the element  $K$  at  $e$ . For the rectangular elements, we would like to take  $\boldsymbol{\beta} = (1, 1)$ .

Next, we would like to base on the above important relationship to prove Lemma 3.1 on both rectangular and triangular elements, respectively. In the following proof, we will focus on the  $\mathcal{P}_k$  finite element space for both cases, and the ‘‘hat’’ terms are related to the information of the reference element  $\hat{K}$ .

### 3.2.1 The proof for rectangular elements

Assume a rectangle  $K = I_i \times J_j$ , where  $I_i = (x_{i-\frac{1}{2}}, x_{i+\frac{1}{2}})$  and  $J_j = (y_{j-\frac{1}{2}}, y_{j+\frac{1}{2}})$ . Let  $\mathbf{q} = (q_1, q_2)$ , then, to prove (3.3), it is sufficient to show that

$$\|u_x\|_K + \sqrt{\mu h^{-1}} \left( \int_{J_j} \llbracket u \rrbracket_{i-\frac{1}{2}, y}^2 dy \right)^{1/2} \leq C_\mu \|q_1\|_K, \quad (3.5a)$$

$$\|u_y\|_K + \sqrt{\mu h^{-1}} \left( \int_{I_i} \llbracket u \rrbracket_{x, j-\frac{1}{2}}^2 dx \right)^{1/2} \leq C_\mu \|q_2\|_K. \quad (3.5b)$$

The proofs for (3.5a) and (3.5b) are similar. In what follows, we only give the proof for (3.5a).

To this end, it is convenient to introduce the reference unit rectangle  $\hat{K} = [0, 1] \times [0, 1]$ , with variables  $\hat{x} = \frac{x-x_{i-\frac{1}{2}}}{h_i}$  and  $\hat{y} = \frac{y-y_{j-\frac{1}{2}}}{h_j}$ , where  $h_i = x_{i+\frac{1}{2}} - x_{i-\frac{1}{2}}$  and  $h_j = y_{j+\frac{1}{2}} - y_{j-\frac{1}{2}}$ . Taking  $\mathbf{r} = (r_1, 0)$  in (3.4), we have

$$(q_1, r_1)_K = (u_x, r_1)_K + \int_{J_j} \llbracket u \rrbracket_{i-\frac{1}{2}, y} r_1(x_{i-\frac{1}{2}}^+, y) dy. \quad (3.6)$$

For any  $v(x, y)$  defined on  $K$ , let  $\hat{v}(\hat{x}, \hat{y}) = v(x, y)$ , then by the change of variable and the chain rule we can get

$$h_i h_j (\hat{q}_1, \hat{r}_1)_{\hat{K}} = h_j (\hat{u}_{\hat{x}}, \hat{r}_1)_{\hat{K}} + h_j \int_0^1 \llbracket \hat{u} \rrbracket_{0, \hat{y}} \hat{r}_1(0^+, \hat{y}) d\hat{y}. \quad (3.7)$$

Choosing  $\hat{r}_1(\hat{x}, \hat{y}) = \hat{x} \hat{u}_{\hat{x}}(\hat{x}, \hat{y})$ , then it is clear that  $\hat{r}_1(0^+, \hat{y}) = 0$ . Thus if we define the weighted norm  $\|\hat{v}\|_{\omega, \hat{K}}^2 \doteq (\hat{v}, \hat{x} \hat{v})_{\hat{K}}$ , which is equivalent to the standard  $L^2$  norm  $\|\hat{v}\|_K$ , then it follows from (3.7) that

$$\|\hat{u}_{\hat{x}}\|_{\omega, \hat{K}}^2 = h_i (\hat{q}_1, \hat{x} \hat{u}_{\hat{x}})_{\hat{K}}.$$

A simple use of the Cauchy-Schwarz inequality leads to

$$\|\hat{u}_{\hat{x}}\|_{\hat{K}} \leq C \|\hat{u}_{\hat{x}}\|_{\omega, \hat{K}} \leq C h_i \|\hat{q}_1\|_{\omega, \hat{K}} \leq C h_i \|\hat{q}_1\|_{\hat{K}}, \quad (3.8)$$

here and below,  $C$  is a generic bounding constant independent of  $h$ .

Next we take  $\hat{r}_1(\hat{x}, \hat{y}) = \hat{u}(\hat{x}, \hat{y}) - \hat{u}(0^-, \hat{y})$ , then  $\hat{r}_1(0^+, \hat{y}) = \llbracket \hat{u} \rrbracket_{0, \hat{y}}$ . Hence, by (3.7) we have

$$\int_0^1 \llbracket \hat{u} \rrbracket_{0, \hat{y}}^2 d\hat{y} = (h_i \hat{q}_1 - \hat{u}_x, \hat{r}_1)_{\hat{K}}.$$

By the Cauchy-Schwarz inequality, (3.8) and the Young's inequality we have

$$\int_0^1 \llbracket \hat{u} \rrbracket_{0,\hat{y}}^2 d\hat{y} \leq C \left[ h_i \|\hat{q}_1\|_{\hat{K}} + \|\hat{u}_x\|_{\hat{K}} \right] \|\hat{r}_1\|_{\hat{K}} \leq \frac{1}{4} \|\hat{r}_1\|_{\hat{K}}^2 + Ch_i^2 \|\hat{q}_1\|_{\hat{K}}^2. \quad (3.9)$$

Noticing that for  $\hat{x} \in [0, 1]$ ,  $\hat{r}_1(\hat{x}, \hat{y}) = \int_0^{\hat{x}} \hat{u}_{\hat{x}}(s, \hat{y}) ds + \llbracket \hat{u} \rrbracket_{0,\hat{y}}$ , then we have

$$\|\hat{r}_1\|_{\hat{K}}^2 \leq 2\|\hat{u}_{\hat{x}}\|_{\hat{K}}^2 + 2 \int_0^1 \llbracket \hat{u} \rrbracket_{0,\hat{y}}^2 d\hat{y}. \quad (3.10)$$

Consequently, owing to (3.8) and (3.9) we get

$$\int_0^1 \llbracket \hat{u} \rrbracket_{0,\hat{y}}^2 d\hat{y} \leq Ch_i^2 \|\hat{q}_1\|_{\hat{K}}^2. \quad (3.11)$$

Finally, by the standard scaling argument we derive (3.5a) from (3.8) and (3.11).

### 3.2.2 The proof for the general triangular elements

For general triangular elements, according to the given direction  $\beta$ , we can divide the triangles into two types: type-I (the left of Figure 1, two *inflow* sides  $e_1, e_2$  and one *outflow* side  $e_3$ ) and type-II (the right of Figure 1, one *inflow* side  $e_1$  and two *outflow* sides  $e_2, e_3$ ).

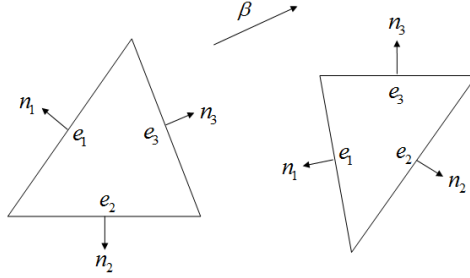


Figure 1: Type-I (left) and Type-II (right) triangles.

In what follows, we will take type-I triangle as an example to prove Lemma 3.1, the proof for type-II triangle is similar and actually much simpler. In order to derive the results, it will be convenient to introduce a reference triangle  $\hat{K}$  with vertices  $\hat{a}_1 = (1, 0)$ ,  $\hat{a}_2 = (0, 1)$  and  $\hat{a}_3 = (0, 0)$ . The reference triangle can be mapped into the triangle  $K$  by the affine transformation [10]

$$\mathbf{x} = R\hat{\mathbf{x}} + \mathbf{a}_3, \quad (3.12)$$

where  $\hat{\mathbf{x}} = (\hat{x}, \hat{y})$  and

$$R = \begin{bmatrix} |\gamma_2|\boldsymbol{\tau}_2 & -|\gamma_1|\boldsymbol{\tau}_1 \end{bmatrix}, \quad (3.13)$$

with  $|\gamma_i|$  being the length of edge  $\gamma_i$  for  $i = 1, 2$ ; see Figure 2. In Figure 2,  $\boldsymbol{\tau}_i$  and  $\mathbf{n}_i$  are the unit tangential and outward normal vectors of edge  $\gamma_i$ , respectively. Obviously, there hold

$$\mathbf{n}_1 = -|\gamma_2|\mathbf{n}_1 \cdot \boldsymbol{\tau}_2 (R^{-1})^\top \hat{\mathbf{n}}_1, \quad \mathbf{n}_2 = -|\gamma_1|\mathbf{n}_1 \cdot \boldsymbol{\tau}_1 (R^{-1})^\top \hat{\mathbf{n}}_2, \quad (3.14)$$

where  $\hat{\mathbf{n}}_1 = (-1, 0)$  and  $\hat{\mathbf{n}}_2 = (0, -1)$ . We also have the following properties of the transformation matrix  $R$ :

- (i)  $R^{-1} = \frac{1}{\mathbf{n}_1 \cdot \boldsymbol{\tau}_2} \begin{pmatrix} \mathbf{n}_1^t / |\gamma_2| \\ \mathbf{n}_2^t / |\gamma_1| \end{pmatrix}$ .
- (ii)  $|\det R| = -\mathbf{n}_1 \cdot \boldsymbol{\tau}_2 |\gamma_1| |\gamma_2| = 2|K|$ , where  $|K|$  is the area of  $K$ .
- (iii)  $\|R\|_2 \leq \sqrt{|\gamma_1|^2 + |\gamma_2|^2}$ , where  $\|R\|_2$  is the  $l^2$ -norm of matrix  $R$ .

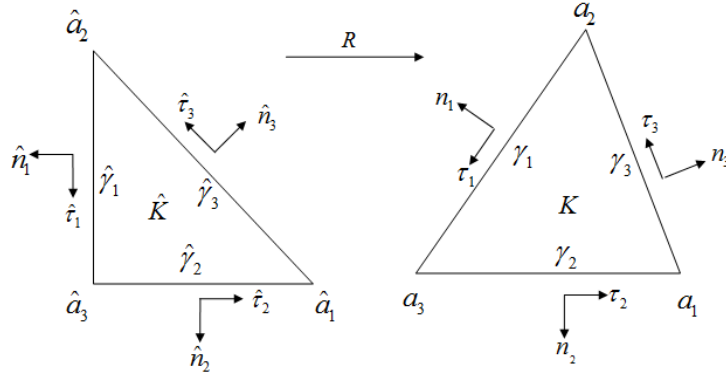


Figure 2: The reference element  $\hat{K}$  and the mapping between  $\hat{K}$  with the element  $K$ .

Let  $\hat{u}(\hat{x}, \hat{y}) = u(x, y)$ ,  $\hat{\mathbf{q}}(\hat{x}, \hat{y}) = \mathbf{q}(x, y)$  and  $\hat{\mathbf{r}}(\hat{x}, \hat{y}) = \mathbf{r}(x, y)$ , then we have

$$\nabla u = (R^{-1})^\top \hat{\nabla} \hat{u}, \quad \text{where } \hat{\nabla} = \begin{pmatrix} \partial / \partial \hat{x} \\ \partial / \partial \hat{y} \end{pmatrix}. \quad (3.15)$$

From (3.4), we have the following relationship for the type-I triangle,

$$(\mathbf{q}, \mathbf{r})_K = (\nabla u, \mathbf{r})_K - \langle \llbracket u \rrbracket, \mathbf{r} \cdot \mathbf{n}_1 \rangle_{\gamma_1} - \langle \llbracket u \rrbracket, \mathbf{r} \cdot \mathbf{n}_2 \rangle_{\gamma_2}, \quad (3.16)$$

then by the change of variables and the chain rule we have

$$\begin{aligned} (\hat{\mathbf{q}}, \hat{\mathbf{r}} | \det R)_{\hat{K}} &= ((R^{-1})^\top \hat{\nabla} \hat{u}, \hat{\mathbf{r}} | \det R)_{\hat{K}} \\ &\quad + \mathbf{n}_1 \cdot \boldsymbol{\tau}_2 |\gamma_1| |\gamma_2| \left( \langle \llbracket \hat{u} \rrbracket, \hat{\mathbf{r}} \cdot (R^{-1})^\top \hat{\mathbf{n}}_1 \rangle_{\hat{\gamma}_1} + \langle \llbracket \hat{u} \rrbracket, \hat{\mathbf{r}} \cdot (R^{-1})^\top \hat{\mathbf{n}}_2 \rangle_{\hat{\gamma}_2} \right). \end{aligned}$$

By property (ii) we get

$$(\hat{\mathbf{q}}, \hat{\mathbf{r}})_{\hat{K}} = ((R^{-1})^\top \hat{\nabla} \hat{u}, \hat{\mathbf{r}})_{\hat{K}} - \langle \llbracket \hat{u} \rrbracket, \hat{\mathbf{r}} \cdot (R^{-1})^\top \hat{\mathbf{n}}_1 \rangle_{\hat{\gamma}_1} - \langle \llbracket \hat{u} \rrbracket, \hat{\mathbf{r}} \cdot (R^{-1})^\top \hat{\mathbf{n}}_2 \rangle_{\hat{\gamma}_2}. \quad (3.17)$$

First we take  $\hat{\mathbf{r}} = R\hat{\mathbf{r}}'$  in (3.17), where

$$\hat{\mathbf{r}}' = (\hat{x} \hat{u}_{\hat{x}}, 0)^\top. \quad (3.18)$$

It is obvious that  $\hat{\mathbf{r}}' = 0$  on  $\hat{\gamma}_1$ , and, since  $\hat{\mathbf{n}}_2 = (0, -1)$ , we have  $\hat{\mathbf{r}}' \cdot \hat{\mathbf{n}}_2 = 0$  on  $\hat{\gamma}_2$ . Hence from (3.17) we get

$$(\hat{\mathbf{q}}, \hat{\mathbf{r}})_{\hat{K}} = ((R^{-1})^\top \hat{\nabla} \hat{u}, \hat{\mathbf{r}})_{\hat{K}} = (\hat{\nabla} \hat{u}, \hat{\mathbf{r}}')_{\hat{K}} = \|\hat{u}_{\hat{x}}\|_{\omega, \hat{K}}^2. \quad (3.19)$$

From (3.13), we get  $\hat{\mathbf{r}} = |\gamma_2| \hat{x} \hat{u}_{\hat{x}} \boldsymbol{\tau}_2$ , then by the Cauchy-Schwarz inequality we get

$$(\hat{\mathbf{q}}, \hat{\mathbf{r}})_{\hat{K}} \leq |\gamma_2| \|\hat{\mathbf{q}}\|_{\omega, \hat{K}} \|\hat{u}_{\hat{x}} \boldsymbol{\tau}_2\|_{\omega, \hat{K}} \leq |\gamma_2| \|\hat{\mathbf{q}}\|_{\omega, \hat{K}} \|\hat{u}_{\hat{x}}\|_{\omega, \hat{K}}, \quad (3.20)$$

here  $\|\hat{\mathbf{q}}\|_{\omega, \hat{K}} = (\hat{\mathbf{q}}, \hat{x} \hat{\mathbf{q}})$ , equivalent to  $\|\hat{\mathbf{q}}\|_{\hat{K}}$ . Hence

$$\|\hat{u}_{\hat{x}}\|_{\hat{K}} \leq C \|\hat{u}_{\hat{x}}\|_{\omega, \hat{K}} \leq Ch \|\hat{\mathbf{q}}\|_{\omega, \hat{K}} \leq Ch \|\hat{\mathbf{q}}\|_{\hat{K}}. \quad (3.21)$$

Similarly, by taking  $\hat{\mathbf{r}} = R \hat{\mathbf{r}}'$  in (3.17), with  $\hat{\mathbf{r}}' = (0, \hat{y} \hat{u}_{\hat{y}})^\top$ , and proceeding in the same way as above we get

$$\|\hat{u}_{\hat{y}}\|_{\hat{K}} \leq Ch \|\hat{\mathbf{q}}\|_{\hat{K}}.$$

Thus

$$\|\hat{\nabla} \hat{u}\|_{\hat{K}} \leq Ch \|\hat{\mathbf{q}}\|_{\hat{K}}. \quad (3.22)$$

Next we take  $\hat{\mathbf{r}} = R \hat{\mathbf{r}}''$  in (3.17), where

$$\hat{\mathbf{r}}'' = \begin{pmatrix} \hat{u} - \hat{u}^-(0, \hat{y}) \\ \hat{u} - \hat{u}^-(\hat{x}, 0) \end{pmatrix}, \quad (3.23)$$

with  $\hat{u}^-(0, \hat{y}) = \lim_{\hat{x} \rightarrow 0^-} \hat{u}(\hat{x}, \hat{y})$  and  $\hat{u}^-(\hat{x}, 0) = \lim_{\hat{y} \rightarrow 0^-} \hat{u}(\hat{x}, \hat{y})$ . Noticing that

$$\hat{\mathbf{r}}''(\hat{x}, \hat{y}) = \begin{pmatrix} \int_0^{\hat{x}} \hat{u}_{\hat{x}}(s, \hat{y}) ds + \llbracket \hat{u} \rrbracket_{\hat{\gamma}_1} \\ \int_0^{\hat{y}} \hat{u}_{\hat{y}}(\hat{x}, s) ds + \llbracket \hat{u} \rrbracket_{\hat{\gamma}_2} \end{pmatrix}, \quad \text{and} \quad \hat{\mathbf{r}}'' \cdot \hat{\mathbf{n}}_i|_{\hat{\gamma}_i} = -\llbracket \hat{u} \rrbracket_{\hat{\gamma}_i}, \quad \text{for } i = 1, 2. \quad (3.24)$$

Thus from (3.17), (3.24) we have

$$\|\llbracket \hat{u} \rrbracket\|_{\hat{\gamma}_1 \cup \hat{\gamma}_2}^2 = (\hat{\mathbf{q}}, \hat{\mathbf{r}})_{\hat{K}} - (\hat{\nabla} \hat{u}, \hat{\mathbf{r}}'')_{\hat{K}}. \quad (3.25)$$

Then a simple use of the Cauchy-Schwarz inequality yields

$$\|\llbracket \hat{u} \rrbracket\|_{\hat{\gamma}_1 \cup \hat{\gamma}_2}^2 \leq \|\hat{\mathbf{q}}\|_{\hat{K}} \|\hat{\mathbf{r}}\|_{\hat{K}} + \|\hat{\nabla} \hat{u}\|_{\hat{K}} \|\hat{\mathbf{r}}''\|_{\hat{K}} \leq \|R\|_2 \|\hat{\mathbf{q}}\|_{\hat{K}} \|\hat{\mathbf{r}}''\|_{\hat{K}} + \|\hat{\nabla} \hat{u}\|_{\hat{K}} \|\hat{\mathbf{r}}''\|_{\hat{K}}.$$

Similar as (3.10), we can get

$$\begin{aligned} \|\hat{\mathbf{r}}''\|_{\hat{K}}^2 &\leq 2(\|\hat{u}_{\hat{x}}\|_{\hat{K}}^2 + \|\llbracket \hat{u} \rrbracket\|_{\hat{\gamma}_1}^2) + 2(\|\hat{u}_{\hat{y}}\|_{\hat{K}}^2 + \|\llbracket \hat{u} \rrbracket\|_{\hat{\gamma}_2}^2) \\ &\leq 2(\|\hat{\nabla} \hat{u}\|_{\hat{K}}^2 + \|\llbracket \hat{u} \rrbracket\|_{\hat{\gamma}_1 \cup \hat{\gamma}_2}^2). \end{aligned}$$

Therefore

$$\|\hat{\mathbf{r}}''\|_{\hat{K}} \leq C(\|\hat{\nabla} \hat{u}\|_{\hat{K}} + \|\llbracket \hat{u} \rrbracket\|_{\hat{\gamma}_1 \cup \hat{\gamma}_2}). \quad (3.26)$$

Hence by (3.22), the property (iii) and (3.26) we get

$$\begin{aligned} \|\llbracket \hat{u} \rrbracket\|_{\hat{\gamma}_1 \cup \hat{\gamma}_2}^2 &\leq Ch \|\hat{\mathbf{q}}\|_{\hat{K}} \|\hat{\mathbf{r}}''\|_{\hat{K}} \\ &\leq Ch \|\hat{\mathbf{q}}\|_{\hat{K}} (h \|\hat{\mathbf{q}}\|_{\hat{K}} + \|\llbracket \hat{u} \rrbracket\|_{\hat{\gamma}_1 \cup \hat{\gamma}_2}) \\ &\leq C_\varepsilon h^2 \|\hat{\mathbf{q}}\|_{\hat{K}}^2 + \varepsilon \|\llbracket \hat{u} \rrbracket\|_{\hat{\gamma}_1 \cup \hat{\gamma}_2}^2, \end{aligned}$$

for arbitrary  $\varepsilon > 0$ , where we have used the Young's inequality in the last line. Hence by choosing  $\varepsilon$  small enough we get

$$\|\llbracket \hat{u} \rrbracket\|_{\hat{\gamma}_1 \cup \hat{\gamma}_2} \leq Ch \|\hat{\mathbf{q}}\|_{\hat{K}}. \quad (3.27)$$

Finally by the scaling argument we obtain

$$\|\nabla u\|_K + h^{-1/2} \|\llbracket u \rrbracket\|_{\gamma_1 \cup \gamma_2} \leq C \|\mathbf{q}\|_K. \quad (3.28)$$

Hence there exists  $C_\mu = C(1 + \sqrt{\mu})$  such that

$$\|\nabla u\|_K + \sqrt{\mu h^{-1}} \|\llbracket u \rrbracket\|_{\gamma_1 \cup \gamma_2} \leq C_\mu \|\mathbf{q}\|_K. \quad (3.29)$$

### 3.3 Elliptic projection in two dimension

In this paper, we would like to use the elliptic projection, to obtain the error estimate of the LDG method, since we are not able to follow the similar line of error analysis in one-dimensional space to obtain the optimal error estimates in multi-dimensional space, because we cannot find a proper projection to eliminate the error at element interface or to make it higher order. This is especially the case for general non-tensor product polynomials of degree  $k$  that we have used, and for the case of triangular rather than rectangular meshes.

For any  $U$  and  $Q = \nabla U$ , the elliptic projection  $(U_h, Q_h)$  is the unique element in  $V_h \times \mathbf{V}_h$ , such that

$$\mathcal{L}(Q, v) = \mathcal{L}(Q_h, v), \quad (3.30a)$$

$$(Q_h, \mathbf{r})_{\Omega_h} = \mathcal{Q}(U_h, \mathbf{r}), \quad (3.30b)$$

hold for any functions  $(v, \mathbf{r}) \in V_h \times \mathbf{V}_h$ . Since in elliptic problems with periodic boundary conditions,  $U_h$  is determined up to an additive constant, we follow [9] to make the assumption

$$(U - U_h, 1)_{\Omega_h} = 0, \quad (3.31)$$

to ensure (3.30) is well-defined.

We have the following approximation property.

**Lemma 3.2.** *There exists the bounding constant  $C$  depending on the regularity of  $U$  and the elliptic regularity constant  $C_*$  to be defined in (3.34), such that*

$$\|U - U_h\| + h^{1/2}\|U - U_h\|_{\Gamma_h} \leq Ch^{k+1}. \quad (3.32)$$

*Proof.* We will finish the proof of this lemma by the aid of two special projections in triangular elements and rectangular elements, which will be studied in the Appendix, and the following adjoint elliptic problem

$$\begin{cases} \psi = \nabla \varphi, \\ \zeta = \nabla \cdot \psi, \end{cases} \quad (3.33)$$

which is assumed to have the following elliptic regularity:

$$\|\psi\|_{H^1(\Omega)} + \|\varphi\|_{H^2(\Omega)} \leq C_* \|\zeta\|_{L^2(\Omega)}. \quad (3.34)$$

Although the proof is lengthy and technical, it is very similar to [9]. We skip the details at present, but for the completeness of this paper, we put the details in the Appendix.  $\square$

## 4 Stability analysis

In this section, we present the stability analysis for the fully discrete IMEX LDG schemes given in Subsection 2.3, on both rectangular elements and triangular elements.

#### 4.1 The properties of the LDG spatial discretization

In this subsection, we will give several lemmas to illustrate some properties of the LDG spatial discretization. All the properties are trivial generalizations of the one-dimensional case [15].

First we consider the linear part. Lemma 4.1 demonstrates the skew symmetric property of the operators  $\mathcal{L}$  and  $\mathcal{Q}$ .

**Lemma 4.1.** *For any  $\mathbf{w} \in \mathbf{V}_h$  and  $v \in V_h$ , there hold the equality*

$$\mathcal{L}(\mathbf{w}, v) = -\mathcal{Q}(v, \mathbf{w}). \quad (4.1)$$

Next we consider the nonlinear operator  $\mathcal{H}$ . Lemma 4.2 states the non-positivity of this operator; we refer to [12] for the proof.

**Lemma 4.2.** *For any  $v \in V_h$ , there hold the inequality*

$$\mathcal{H}(v, v) \leq 0. \quad (4.2)$$

The next lemma states the boundedness properties of the nonlinear operator  $\mathcal{H}$ . To this end, we would like to assume that the numerical flux  $\tilde{F}_{\mathbf{n}_K, K}$  is locally Lipschitz continuous with respect to each component, and we denote the Lipschitz constant as  $C_f$ . Then we have

$$|\tilde{F}_{\mathbf{n}_K, K}(a, b) - \tilde{F}_{\mathbf{n}_K, K}(c, d)| \leq C_f(|a - c| + |b - d|), \quad (4.3a)$$

for arbitrary  $a, b, c, d$  and arbitrary  $K$ , which implies

$$|f'(p)| \leq C_f, \quad |g'(p)| \leq C_f, \quad \forall p, \quad (4.3b)$$

if both  $f$  and  $g$  are differentiable.

**Lemma 4.3.** *For any  $u, w, v \in V_h$ , there hold the following inequalities*

$$|\mathcal{H}(u, v)| \leq C_f \left( \|\nabla u\| + \sqrt{\mu h^{-1}} \|[[u]]\|_{\Gamma_h} \right) \|v\|, \quad (4.4)$$

$$|\mathcal{D}(u, w; v)| \leq C_f \|u - w\| \left( \|\nabla v\| + \sqrt{\mu h^{-1}} \|[[v]]\|_{\Gamma_h} \right), \quad (4.5)$$

if (4.3) holds. Here

$$\mathcal{D}(u, w; v) = \mathcal{H}(u, v) - \mathcal{H}(w, v). \quad (4.6)$$

*Proof.* The proof is the simple generalization of the proof of Lemma 3.3 in [15] for the one-dimensional case. We omit the detailed proof here; see [15] for more details.  $\square$

#### 4.2 The main conclusion

Owing to the properties we studied in Subsections 3.2 and 4.1, we can easily generalize the stability result in [15] for the one-dimensional convection-diffusion problems to the multi-dimensional cases.

**Theorem 4.1.** *There exists a positive constant  $\tau_0$  independent of  $h$ , such that if  $\tau \leq \tau_0$ , then the solutions of schemes (2.10), (2.11) and (2.12) satisfy*

$$\|u^n\| \leq \|u^0\|, \quad \forall n, \quad (4.7)$$

if (4.3) holds.

*Proof.* Since the stability property on multi-dimension spaces is very similar to the one-dimensional case, we only take the second order scheme (2.11) as an example to prove it, and refer to [14] and [15] for more details about the proof for the first and third order schemes.

From (2.11a) and (2.11b), we get

$$(u^{n,1} - u^n, v)_{\Omega_h} = \gamma\tau\mathcal{H}(u^n, v) + \gamma\tau\mathcal{L}(\mathbf{q}^{n,1}, v), \quad (4.8a)$$

$$\begin{aligned} (u^{n+1} - u^{n,1}, v)_{\Omega_h} &= (\delta - \gamma)\tau\mathcal{H}(u^n, v) + (1 - \delta)\tau\mathcal{H}(u^{n,1}, v) \\ &\quad + (1 - 2\gamma)\tau\mathcal{L}(\mathbf{q}^{n,1}, v) + \gamma\tau\mathcal{L}(\mathbf{q}^{n+1}, v). \end{aligned} \quad (4.8b)$$

By taking  $v = u^{n,1}, u^{n+1}$  in (4.8a) and (4.8b), respectively, and adding them together, we obtain

$$\underbrace{\frac{1}{2}\|u^{n+1}\|^2 - \frac{1}{2}\|u^n\|^2 + \frac{1}{2}\|u^{n+1} - u^{n,1}\|^2 + \frac{1}{2}\|u^{n,1} - u^n\|^2}_{LHS} = R_1 + R_2,$$

where

$$\begin{aligned} R_1 &= \gamma\tau\mathcal{H}(u^n, u^{n,1}) + (\delta - \gamma)\tau\mathcal{H}(u^n, u^{n+1}) + (1 - \delta)\tau\mathcal{H}(u^{n,1}, u^{n+1}), \\ R_2 &= \gamma\tau\mathcal{L}(\mathbf{q}^{n,1}, u^{n,1}) + (1 - 2\gamma)\tau\mathcal{L}(\mathbf{q}^{n,1}, u^{n+1}) + \gamma\tau\mathcal{L}(\mathbf{q}^{n+1}, u^{n+1}). \end{aligned}$$

Owing to (4.1) and (2.11c), we have

$$\begin{aligned} R_2 &= -\gamma\tau\mathcal{Q}(u^{n,1}, \mathbf{q}^{n,1}) - (1 - 2\gamma)\tau\mathcal{Q}(u^{n+1}, \mathbf{q}^{n,1}) - \gamma\tau\mathcal{Q}(u^{n+1}, \mathbf{q}^{n+1}) \\ &= -\gamma\tau\|\mathbf{q}^{n,1}\|^2 - (1 - 2\gamma)\tau(\mathbf{q}^{n,1}, \mathbf{q}^{n+1})_{\Omega_h} - \gamma\tau\|\mathbf{q}^{n+1}\|^2. \end{aligned} \quad (4.9)$$

In order to use the stability terms provided by  $LHS$  and  $R_2$  to estimate  $R_1$ , we rewrite  $R_1$  in the following equivalent form:

$$\begin{aligned} R_1 &= \gamma\tau\mathcal{H}(u^{n,1}, u^{n,1}) + (1 - \gamma)\tau\mathcal{H}(u^{n+1}, u^{n+1}) - \gamma\tau\mathcal{D}(u^{n,1}, u^n; u^{n,1}) \\ &\quad - (1 - \gamma)\tau\mathcal{D}(u^{n+1}, u^{n,1}; u^{n+1}) - (\delta - \gamma)\tau\mathcal{D}(u^{n,1}, u^n; u^{n+1}). \end{aligned}$$

Noting that  $\delta - \gamma = -1$ , and by the property (4.2) we have

$$R_1 \leq -\gamma\tau\mathcal{D}(u^{n,1}, u^n; u^{n,1}) - (1 - \gamma)\tau\mathcal{D}(u^{n+1}, u^{n,1}; u^{n+1}) + \tau\mathcal{D}(u^{n,1}, u^n; u^{n+1}).$$

Exploiting (4.5), Lemma 3.1 and the Young's inequality successively, we can derive

$$\begin{aligned} R_1 &\leq C_f(\|u^{n,1} - u^n\| + \|u^{n+1} - u^{n,1}\|) \sum_{\ell=1}^2 (\|\nabla u^{n,\ell}\| + \sqrt{\mu h^{-1}} \|[u^{n,\ell}]\|_{\Gamma_h}) \\ &\leq C_f C_\mu (\|u^{n,1} - u^n\| + \|u^{n+1} - u^{n,1}\|) (\|\mathbf{q}^{n,1}\| + \|\mathbf{q}^{n+1}\|) \\ &\leq \frac{\gamma}{4}\tau(\|\mathbf{q}^{n,1}\|^2 + \|\mathbf{q}^{n+1}\|^2) + C_f C_\mu^2 \tau (\|u^{n,1} - u^n\|^2 + \|u^{n+1} - u^{n,1}\|^2), \end{aligned}$$

here and below we use  $C_f$  to denote a generic bounding constant which is independent of  $h$  and  $\tau$ . As a consequence, we obtain

$$LHS + S \leq C_f C_\mu^2 \tau (\|u^{n,1} - u^n\|^2 + \|u^{n+1} - u^{n,1}\|^2),$$

where

$$\begin{aligned} S &= \frac{3}{4} \gamma \tau \|\mathbf{q}^{n,1}\|^2 + (1 - 2\gamma) \tau (\mathbf{q}^{n,1}, \mathbf{q}^{n+1})_{\Omega_h} + \frac{3}{4} \gamma \tau \|\mathbf{q}^{n+1}\|^2 \\ &\geq [\frac{3}{4} \gamma - (\frac{1}{2} - \gamma)] \tau (\|\mathbf{q}^{n,1}\|^2 + \|\mathbf{q}^{n+1}\|^2) \geq 0, \end{aligned} \quad (4.10)$$

owing to the setting of  $\gamma$  and the Young's inequality. Then

$$LHS \leq C_f C_\mu^2 \tau (\|u^{n,1} - u^n\|^2 + \|u^{n+1} - u^{n,1}\|^2).$$

Consequently, if  $C_f C_\mu^2 \tau \leq \frac{1}{2}$ , i.e.,  $\tau \leq \tau_0 = \frac{1}{2C_f C_\mu^2}$ , then we obtain (4.7).  $\square$

*Remark 4.1.* In Theorem 4.1,  $\tau_0$  may have different values for the three schemes. In this paper we use  $\tau_0$  as a generic bound of the time step, which may have different values in each occurrence.

## 5 Error estimates

To obtain the optimal error estimates for the IMEX LDG schemes introduced in Subsection 2.3, we would like to assume that the exact solution  $U(\mathbf{x}, t)$  is sufficiently smooth, for example, for  $s$ -th order fully discrete IMEX LDG schemes (2.10), (2.11) or (2.12), we assume

$$U(\mathbf{x}, t) \in L^\infty(0, T; H^{k+2}), \quad D_t U(\mathbf{x}, t) \in L^\infty(0, T; H^{k+1}), \quad (5.1a)$$

and

$$D_t^{s+1} U(\mathbf{x}, t) \in L^\infty(0, T; L^2), \quad (5.1b)$$

for  $s = 1, 2, 3$ , where  $D_t^\ell U$  means the  $\ell$ -th order time derivative of  $U$ , and the notation  $L^\infty(0, T; H^s(D))$  represents the set of functions  $v$  such that  $\max_{0 \leq t \leq T} \|v(\cdot, t)\|_{H^s(D)} < \infty$ .

We give the main results in the following theorem.

**Theorem 5.1.** *Let  $U(\mathbf{x}, t)$  be the exact solution of (1.1), satisfying the smoothness assumption (5.1), let  $u^n \in V_h$  be the solution of the  $s$ -th order fully discrete IMEX LDG schemes (2.10), (2.11) or (2.12). Then there exists a positive constant  $\tau_0$  independent of the spatial size  $h$ , such that if  $\tau \leq \tau_0$  then*

$$\max_{n\tau \leq T} \|U(\mathbf{x}, t^n) - u^n\| \leq C(h^{k+1} + \tau^s), \quad (5.2)$$

for  $s = 1, 2, 3$ , where  $T$  is the final computing time and the bounding constant  $C > 0$  is independent of  $h$  and  $\tau$ .

*Remark 5.1.* To derive the optimal error estimate, we would like to follow [9] to make use of the so-called *elliptic projections* [13, 17]. To make the idea clear enough, we would like to take the second order scheme (2.11) as an example to finish the proof. The same idea can be used for the first order scheme (2.10) and the third order scheme (2.12). In addition, for the third order scheme, we also need to adopt the technique used in [24, 25], i.e, we need to make the *a priori* error assumption, since there is one more explicit stage than the implicit stage in our third order scheme (2.12), there will appear a trouble term which makes the analysis much more technical. For more details, please refer to [15].

In the following subsections, we will pay our attention to the proof for Theorem 5.1 on both rectangular and triangular elements, for the second order IMEX LDG method (2.11).

### 5.1 Reference functions and error splitting

Following [24, 25, 14], we define two reference functions of (2.2) as follow: let  $U^{(0)} = U$  be the exact solution of the problem (1.1), then define

$$U^{(1)} = U^{(0)} - \gamma\tau\nabla \cdot \mathbf{F}(U^{(0)}) + \gamma\tau\nabla \cdot \mathbf{Q}^{(1)}, \quad (5.3a)$$

where

$$\mathbf{Q}^{(1)} = \nabla U^{(1)}. \quad (5.3b)$$

For any indexes  $n$  and  $\ell$  under consideration, the reference function at each stage time level is defined as  $(U^{n,\ell}, \mathbf{Q}^{n,\ell}) = (U^{(\ell)}(\mathbf{x}, t^n), \mathbf{Q}^{(\ell)}(\mathbf{x}, t^n))$ . If  $\ell = 0$ , we drop the superscript  $\ell$ .

In what follows, we would like to denote the stage error by

$$(e_u^{n,\ell}, e_{\mathbf{q}}^{n,\ell}) = (U^{n,\ell} - u^{n,\ell}, \mathbf{Q}^{n,\ell} - \mathbf{q}^{n,\ell}), \quad \text{for } \ell = 0, 1, \quad (5.4)$$

and divide it in two parts, namely,

$$(e_u^{n,\ell}, e_{\mathbf{q}}^{n,\ell}) = (\xi_u^{n,\ell} - \eta_u^{n,\ell}, \xi_{\mathbf{q}}^{n,\ell} - \eta_{\mathbf{q}}^{n,\ell}), \quad (5.5)$$

where

$$(\xi_u^{n,\ell}, \xi_{\mathbf{q}}^{n,\ell}) = (U_h^{n,\ell} - u^{n,\ell}, \mathbf{Q}_h^{n,\ell} - \mathbf{q}^{n,\ell}), \quad (\eta_u^{n,\ell}, \eta_{\mathbf{q}}^{n,\ell}) = (U_h^{n,\ell} - U^{n,\ell}, \mathbf{Q}_h^{n,\ell} - \mathbf{Q}^{n,\ell}), \quad (5.6)$$

with  $(U_h^{n,\ell}, \mathbf{Q}_h^{n,\ell})$  being the elliptic projection of  $(U^{n,\ell}, \mathbf{Q}^{n,\ell})$ , namely

$$\mathcal{L}(\mathbf{Q}^{n,\ell}, v) = \mathcal{L}(\mathbf{Q}_h^{n,\ell}, v), \quad (5.7a)$$

$$(\mathbf{Q}_h^{n,\ell}, \mathbf{r})_{\Omega_h} = \mathcal{Q}(U_h^{n,\ell}, \mathbf{r}), \quad (5.7b)$$

hold for any functions  $(v, \mathbf{r}) \in V_h \times \mathbf{V}_h$ ; see Subsection 3.3.

Owing to the linear structure of elliptic projection and Lemma 3.2, we have the following approximation properties

$$\|\eta_u^{n,\ell}\| + h^{1/2}\|\eta_{\mathbf{q}}^{n,\ell}\|_{\Gamma_h} \leq Ch^{k+1}, \quad (5.8)$$

and

$$\|\eta_u^{n,\ell} - \eta_u^n\| \leq Ch^{k+1}\tau, \quad (5.9)$$

where  $C$  only depends on the regularity of  $U$  and the elliptic regularity constant  $C_*$  which is defined in (3.34).

## 5.2 The error equations and the energy equation

To estimate  $\xi_u^{n,\ell}$ , we need to set up the corresponding error equations. For the second order time-marching, it is easy to verify that

$$U^{n+1} = U^n - \delta\tau\nabla \cdot \mathbf{F}(U^n) - (1-\delta)\tau\nabla \cdot \mathbf{F}(U^{n,1}) + (1-\gamma)\tau\nabla \cdot \mathbf{Q}^{n,1} + \gamma\tau\nabla \cdot \mathbf{Q}^{n+1} + \zeta^n, \quad (5.10)$$

where  $\mathbf{Q}^{n+1} = \nabla U^{n+1}$ , and  $\zeta^n$  is the local truncation error satisfying

$$\|\zeta^n\| \leq C\tau^3, \quad (5.11)$$

with the bounding constant  $C$  only depending on the regularity of the exact solution  $U$ .

Thanks to the smoothness assumption (5.1), we know that  $\mathbf{F}(U^{n,\ell})$  and  $\mathbf{Q}^{n,\ell}$  are continuous functions. Then it follows from (5.3), (5.7) and (5.10) that

$$(U^{n,1} - U^n, v)_{\Omega_h} = \gamma\tau\mathcal{H}(U^n, v) + \gamma\tau\mathcal{L}(\mathbf{Q}_h^{n,1}, v), \quad (5.12a)$$

$$\begin{aligned} (U^{n+1} - U^n, v)_{\Omega_h} &= \delta\tau\mathcal{H}(U^n, v) + (1-\delta)\tau\mathcal{H}(U^{n,1}, v) \\ &\quad + (1-\gamma)\tau\mathcal{L}(\mathbf{Q}_h^{n,1}, v) + \gamma\tau\mathcal{L}(\mathbf{Q}_h^{n+1}, v) + (\zeta^n, v)_{\Omega_h}, \end{aligned} \quad (5.12b)$$

and

$$(\mathbf{Q}^{n,\ell}, \mathbf{r})_{\Omega_h} = \mathcal{Q}(U^{n,\ell}, \mathbf{r}), \quad \text{for } \ell = 1, 2. \quad (5.12c)$$

Here and below,  $\mathbf{Q}^{n,2} = \mathbf{Q}^{n+1}$  and  $U^{n,2} = U^{n+1}$ . Hence, subtracting (2.11) from (5.12) gives rise to the error equations: for all  $v \in V_h$ ,

$$(\xi_u^{n,1} - \xi_u^n, v)_{\Omega_h} = (\eta_u^{n,1} - \eta_u^n, v)_{\Omega_h} + \gamma\tau\mathcal{D}(U^n, u^n; v) + \gamma\tau\mathcal{L}(\xi_q^{n,1}, v), \quad (5.13a)$$

$$\begin{aligned} (\xi_u^{n+1} - \xi_u^n, v)_{\Omega_h} &= (\eta_u^{n+1} - \eta_u^n, v)_{\Omega_h} + \delta\tau\mathcal{D}(U^n, u^n; v) + (1-\delta)\tau\mathcal{D}(U^{n,1}, u^{n,1}; v) \\ &\quad + (1-\gamma)\tau\mathcal{L}(\xi_q^{n,1}, v) + \gamma\tau\mathcal{L}(\xi_q^{n+1}, v) + (\zeta^n, v)_{\Omega_h}. \end{aligned} \quad (5.13b)$$

From (2.11c) and (5.7b) we get: for all  $\mathbf{r} \in \mathbf{V}_h$ ,

$$(\xi_q^{n,\ell}, \mathbf{r})_{\Omega_h} = \mathcal{Q}(\xi_u^{n,\ell}, \mathbf{r}), \quad \text{for } \ell = 1, 2. \quad (5.13c)$$

Next we would like to obtain the energy equation for  $\xi_u^{n,\ell}$ . To this end, we subtract (5.13a) from (5.13b), and get

$$\begin{aligned} (\xi_u^{n+1} - \xi_u^{n,1}, v)_{\Omega_h} &= (\eta_u^{n+1} - \eta_u^{n,1}, v)_{\Omega_h} + (\delta - \gamma)\tau\mathcal{D}(U^n, u^n; v) + (1-\delta)\tau\mathcal{D}(U^{n,1}, u^{n,1}; v) \\ &\quad + (1-2\gamma)\tau\mathcal{L}(\xi_q^{n,1}, v) + \gamma\tau\mathcal{L}(\xi_q^{n+1}, v) + (\zeta^n, v)_{\Omega_h}. \end{aligned} \quad (5.14)$$

Taking  $v = \xi_u^{n,1}, \xi_u^{n+1}$  in (5.13a) and (5.14) respectively, and adding them together, we can derive the energy equation

$$\frac{1}{2}\|\xi_u^{n+1}\|^2 - \frac{1}{2}\|\xi_u^n\|^2 + \frac{1}{2}\|\xi_u^{n+1} - \xi_u^{n,1}\|^2 + \frac{1}{2}\|\xi_u^{n,1} - \xi_u^n\|^2 = \mathcal{T}_p + \mathcal{T}_d + \mathcal{T}_c, \quad (5.15)$$

where

$$\begin{aligned} \mathcal{T}_p &= (\eta_u^{n,1} - \eta_u^n, \xi_u^{n,1})_{\Omega_h} + (\eta_u^{n+1} - \eta_u^{n,1}, \xi_u^{n+1})_{\Omega_h} + (\zeta^n, \xi_u^{n+1})_{\Omega_h}, \\ \mathcal{T}_d &= \gamma\tau\mathcal{L}(\xi_q^{n,1}, \xi_u^{n,1}) + (1-2\gamma)\tau\mathcal{L}(\xi_q^{n,1}, \xi_u^{n+1}) + \gamma\tau\mathcal{L}(\xi_q^{n+1}, \xi_u^{n+1}), \\ \mathcal{T}_c &= \gamma\tau\mathcal{D}(U^n, u^n; \xi_u^{n,1}) + (\delta - \gamma)\tau\mathcal{D}(U^n, u^n; \xi_u^{n+1}) + (1-\delta)\tau\mathcal{D}(U^{n,1}, u^{n,1}; \xi_u^{n+1}). \end{aligned}$$

In the next subsection we will estimate them separately.

### 5.3 Energy estimate

The estimate for the first two terms is easy. A simple use of the Cauchy-Schwarz inequality, the Young's inequality and (5.9), (5.11) leads to

$$\mathcal{T}_p \leq \varepsilon \tau (\|\xi_u^{n,1}\|^2 + \|\xi_u^{n+1}\|^2) + C_\varepsilon (h^{2k+2} \tau + \tau^5),$$

for arbitrary  $\varepsilon > 0$ . Then choosing  $\varepsilon$  small enough and using the triangle inequality we get

$$\mathcal{T}_p \leq \tau (\|\xi_u^n\|^2 + \|\xi_u^{n,1} - \xi_u^n\|^2 + \|\xi_u^{n+1} - \xi_u^{n,1}\|^2) + C(h^{2k+2} \tau + \tau^5). \quad (5.16)$$

By (4.1) and (5.13c) we have

$$\begin{aligned} \mathcal{T}_d &= -\gamma \tau \mathcal{Q}(\xi_u^{n,1}, \xi_q^{n,1}) - (1-2\gamma) \tau \mathcal{Q}(\xi_u^{n+1}, \xi_q^{n,1}) - \gamma \tau \mathcal{Q}(\xi_u^{n+1}, \xi_q^{n+1}) \\ &= -\gamma \tau \|\xi_q^{n,1}\|^2 - (1-2\gamma) \tau (\xi_q^{n,1}, \xi_q^{n+1})_{\Omega_h} - \gamma \tau \|\xi_q^{n+1}\|^2. \end{aligned} \quad (5.17)$$

The estimate for  $\mathcal{T}_c$  is a bit more complex. Due to (2.5a), we have

$$\begin{aligned} \mathcal{D}(U^{n,\ell}, u^{n,\ell}; v) &= \sum_{K \in \Omega_h} (\mathbf{F}(U^{n,\ell}) - \mathbf{F}(u^{n,\ell}), \nabla v)_K \\ &\quad - \sum_{K \in \Omega_h} \langle \tilde{F}_{\mathbf{n}_K, K}((U^{n,\ell})^{int_K}, (U^{n,\ell})^{ext_K}) - \tilde{F}_{\mathbf{n}_K, K}((u^{n,\ell})^{int_K}, (u^{n,\ell})^{ext_K}), [v] \rangle_{\partial \bar{K}}, \end{aligned}$$

then we can get the upper bound of this term along the similar line as the proof for Lemma 4.3. By the Lipschitz continuity and the assumption (4.3) we have

$$\mathcal{D}(U^{n,\ell}, u^{n,\ell}; v) \leq C_f \|U^{n,\ell} - u^{n,\ell}\| \|\nabla v\| + C_f \|U^{n,\ell} - u^{n,\ell}\|_{\Gamma_h} \|[v]\|_{\Gamma_h}. \quad (5.18)$$

By the triangle inequality we have

$$\begin{aligned} \|U^{n,\ell} - u^{n,\ell}\| &\leq \|\xi_u^{n,\ell}\| + \|\eta_u^{n,\ell}\| \leq \|\xi_u^{n,\ell}\| + Ch^{k+1}, \\ \|U^{n,\ell} - u^{n,\ell}\|_{\Gamma_h} &\leq \|\xi_u^{n,\ell}\|_{\Gamma_h} + \|\eta_u^{n,\ell}\|_{\Gamma_h} \leq \sqrt{\mu h^{-1}} (\|\xi_u^{n,\ell}\| + Ch^{k+1}), \end{aligned}$$

where we have used the approximation property (5.8) and the inverse property (3.1). Thus we get the desired result

$$|\mathcal{D}(U^{n,\ell}, u^{n,\ell}; v)| \leq C_f (\|\xi_u^{n,\ell}\| + h^{k+1}) (\|\nabla v\| + \sqrt{\mu h^{-1}} \|[v]\|_{\Gamma_h}). \quad (5.19)$$

Furthermore, owing to (5.13c) and proceeding in the similar line as in the proof of Lemma 3.1, we can get

$$\|\nabla \xi_u^{n,\ell}\| + \sqrt{\mu h^{-1}} \|[ \xi_u^{n,\ell} ]\|_{\Gamma_h} \leq C_\mu \|\xi_q^{n,\ell}\|. \quad (5.20)$$

As a consequence, by applying (5.19) and (5.20) we obtain

$$\begin{aligned} \mathcal{T}_c &\leq C_f \tau (\|\xi_u^n\| + \|\xi_u^{n,1}\| + h^{k+1}) \sum_{\ell=1}^2 (\|\nabla \xi_u^{n,\ell}\| + \sqrt{\mu h^{-1}} \|[ \xi_u^{n,\ell} ]\|_{\Gamma_h}) \\ &\leq C_f C_\mu \tau (\|\xi_u^n\| + \|\xi_u^{n,1}\| + h^{k+1}) (\|\xi_q^{n,1}\| + \|\xi_q^{n+1}\|). \end{aligned}$$

Then a simple application of the triangle inequality and the Young's inequality yields

$$\begin{aligned} \mathcal{T}_c &\leq C_f C_\mu \tau (2\|\xi_u^n\| + \|\xi_u^{n,1} - \xi_u^n\| + h^{k+1})(\|\xi_q^{n,1}\| + \|\xi_q^{n+1}\|) \\ &\leq \frac{\gamma}{4}\tau(\|\xi_q^{n,1}\|^2 + \|\xi_q^{n+1}\|^2) + C_f C_\mu^2 \tau \|\xi_u^{n,1} - \xi_u^n\|^2 + C\tau\|\xi_u^n\|^2 + Ch^{2k+2}\tau. \end{aligned} \quad (5.21)$$

Thus by (5.16), (5.17), and (5.21) we can derive

$$\mathcal{T}_p + \mathcal{T}_d + \mathcal{T}_c \leq \mathcal{S}_2 - \mathcal{S}_1 + C\tau\|\xi_u^n\|^2 + C(h^{2k+2}\tau + \tau^5), \quad (5.22)$$

where

$$\begin{aligned} \mathcal{S}_1 &= \frac{3}{4}\gamma\tau\|\xi_q^{n,1}\|^2 + (1 - 2\gamma)\tau(\xi_q^{n,1}, \xi_q^{n+1})_{\Omega_h} + \frac{3}{4}\gamma\tau\|\xi_q^{n+1}\|^2, \\ \mathcal{S}_2 &= (C_f C_\mu^2 + 1)\tau(\|\xi_u^{n,1} - \xi_u^n\|^2 + \|\xi_u^{n+1} - \xi_u^{n,1}\|^2). \end{aligned}$$

Then, similar as (4.10), we have  $\mathcal{S}_1 \geq 0$ , hence, if  $(C_f C_\mu^2 + 1)\tau \leq \frac{1}{2}$ , i.e,  $\tau \leq \tau_0 \leq \frac{1}{2(C_f C_\mu^2 + 1)}$ , it follows from (5.15) that

$$\|\xi_u^{n+1}\|^2 - \|\xi_u^n\|^2 \leq C\tau\|\xi_u^n\|^2 + C(h^{2k+2}\tau + \tau^5). \quad (5.23)$$

Consequently, by the discrete Gronwall inequality we arrive at

$$\|\xi_u^n\| \leq C(h^{k+1} + \tau^2). \quad (5.24)$$

Finally, by (5.8), (5.24) and the triangle inequality we obtain (5.2) with  $s = 2$ . Thus we have completed the proof of Theorem 5.1 with  $s = 2$ .  $\square$

## 6 Numerical experiments

In this section, we will first numerically validate the orders of accuracy for the second order IMEX LDG scheme (2.11) and the third order IMEX LDG scheme (2.12), then we will verify the stability of the two schemes. For the third order IMEX LDG scheme (2.12), we take the parameter  $\alpha_1 = -0.35$  as done in [3].

In what follows, we will test the following two examples to verify the orders of accuracy for the two schemes on both rectangular elements and triangular elements. We will test each example for  $\nu = 1, 0.1, 0.01$  and  $10^{-5}$ . In all the experiments, the final time is  $T = 1$  and we take the time step  $\tau = \lambda h$ , where  $h$  is the mesh size and we take  $\lambda = 0.5$  for  $\nu = 1$ ,  $\lambda = 0.3$  for  $\nu = 0.1$  and  $\lambda = 0.1$  for both  $\nu = 0.01$  and  $\nu = 10^{-5}$ .

*Example 1.*

$$\begin{cases} U_t + U_x + U_y = \nu(U_{xx} + U_{yy}), \\ U(x, y, 0) = \sin(x + y), \end{cases} \quad (6.1)$$

on  $(x, y) \in [-\pi, \pi] \times [-\pi, \pi]$ . The exact solution is

$$U(x, y, t) = e^{-2\nu t} \sin(x + y - 2t). \quad (6.2)$$

*Example 2.*

$$\begin{cases} U_t + \left(\frac{U^2}{2}\right)_x + \left(\frac{U^2}{2}\right)_y = \nu(U_{xx} + U_{yy}) + f(x, y, t), \\ U(x, y, 0) = \sin(x + y), \end{cases} \quad (6.3)$$

on  $(x, y) \in [-\pi, \pi] \times [-\pi, \pi]$ , where  $f(x, y, t) = e^{-4\nu t} \sin(2(x + y))$ . The exact solution is

$$U(x, y, t) = e^{-2\nu t} \sin(x + y). \quad (6.4)$$

In Table 1, we list the  $L^2$  errors and orders of accuracy for the IMEX LDG schemes (2.11) and (2.12) for solving the above two examples on nonuniform rectangular meshes. The nonuniform rectangular meshes are obtained by randomly perturbing each node in the uniform mesh by up to 20%. In all the tests, we take  $h = \min\{2\pi/nx, 2\pi/ny\}$ , where  $nx$  and  $ny$  are the numbers of partition in the  $x$  and  $y$  directions, respectively.

Table 1: Errors and orders of accuracy on nonuniform rectangular elements.

<b>Example 1</b>		$\nu = 1$		$\nu = 0.1$		$\nu = 0.01$		$\nu = 10^{-5}$	
scheme	$(nx, ny)$	$L^2$ error	order	$L^2$ error	order	$L^2$ error	order	$L^2$ error	order
$\mathcal{P}_1$ IMEX RK2	(10,10)	8.25E-01	-	1.31E+00	-	1.30E+00	-	1.31E+00	-
	(20,20)	1.88E-01	2.13	3.37E-01	1.96	3.23E-01	2.00	3.30E-01	1.99
	(40,40)	4.56E-02	2.04	8.58E-02	1.97	8.13E-02	1.99	8.34E-02	1.99
	(80,80)	1.12E-02	2.02	2.15E-02	1.99	2.05E-02	1.99	2.11E-02	1.98
	(160,160)	2.79E-03	2.01	5.41E-03	1.99	5.15E-03	1.99	5.25E-03	1.99
$\mathcal{P}_2$ IMEX RK3	(10,10)	1.47E-01	-	1.99E-01	-	1.61E-01	-	1.66E-01	-
	(20,20)	2.15E-02	2.77	1.84E-02	3.44	2.02E-02	2.99	2.05E-02	3.01
	(40,40)	2.99E-03	2.85	2.27E-03	3.02	2.53E-03	3.00	2.60E-03	2.98
	(80,80)	3.98E-04	2.91	2.84E-04	3.00	3.16E-04	3.00	3.25E-04	3.00
	(160,160)	5.16E-05	2.95	3.56E-05	3.00	3.96E-05	3.00	4.07E-05	3.00
<b>Example 2</b>		$\nu = 1$		$\nu = 0.1$		$\nu = 0.01$		$\nu = 10^{-5}$	
scheme	$(nx, ny)$	$L^2$ error	order	$L^2$ error	order	$L^2$ error	order	$L^2$ error	order
$\mathcal{P}_1$ IMEX RK2	(10,10)	1.96E-01	-	1.02E+00	-	1.28E+00	-	1.33E+00	-
	(20,20)	4.87E-02	2.01	2.55E-01	2.00	3.09E-01	2.05	3.27E-01	2.02
	(40,40)	1.21E-02	2.01	6.51E-02	1.97	7.57E-02	2.03	8.07E-02	2.02
	(80,80)	3.00E-03	2.01	1.67E-02	1.97	1.88E-02	2.01	2.04E-02	1.98
	(160,160)	7.51E-04	2.00	4.23E-03	1.98	4.76E-03	1.98	4.98E-03	1.99
$\mathcal{P}_2$ IMEX RK3	(10,10)	3.50E-02	-	1.12E-01	-	1.32E-01	-	1.39E-01	-
	(20,20)	4.90E-03	2.84	1.48E-02	2.93	1.60E-02	3.05	1.82E-02	2.93
	(40,40)	6.65E-04	2.88	1.94E-03	2.93	1.97E-03	3.02	2.34E-03	2.96
	(80,80)	8.70E-05	2.94	2.52E-04	2.95	2.51E-04	2.97	3.10E-04	2.91
	(160,160)	1.12E-05	2.96	3.23E-05	2.96	3.32E-05	2.92	4.03E-05	2.94

In Table 2, we list the  $L^2$  errors and orders of accuracy for the IMEX LDG schemes (2.11) and (2.12) for solving the above two examples on general triangular meshes. In all the tests, we take  $h = \min_K \{\sqrt{|K|}\}$ , where  $|K|$  is the area of the triangle element  $K$ . In our experiments, the initial mesh is in Figure 3, and in each refinement, every triangle is subdivided to four children triangles by joining the mid-points of the edges of it.

From these tables, we can clearly observe optimal orders of accuracy for our schemes on both nonuniform rectangular meshes and the general triangular meshes.

Table 2: Errors and orders accuracy on general triangular elements.

<b>Example 1</b>		$\nu = 1$		$\nu = 0.1$		$\nu = 0.01$		$\nu = 10^{-5}$	
scheme	refine	$L^2$ error	order	$L^2$ error	order	$L^2$ error	order	$L^2$ error	order
$\mathcal{P}_1$ IMEX RK2	1	2.32E-01	-	4.68E-01	-	4.74E-01	-	4.82E-01	-
	2	5.55E-02	2.06	1.17E-01	2.01	1.23E-01	1.94	1.26E-01	1.93
	3	1.40E-02	1.99	2.86E-02	2.03	3.10E-02	2.00	3.20E-02	1.98
	4	3.39E-03	2.04	7.10E-03	2.01	7.66E-03	2.02	8.00E-03	2.00
	5	8.33E-04	2.02	1.77E-03	2.01	1.88E-03	2.03	2.00E-03	2.00
$\mathcal{P}_2$ IMEX RK3	1	4.00E-02	-	6.43E-02	-	6.79E-02	-	6.99E-02	-
	2	6.23E-03	2.68	7.15E-03	3.17	8.30E-03	3.03	8.46E-03	3.05
	3	9.22E-04	2.76	8.94E-04	3.00	1.04E-03	3.00	1.04E-03	3.03
	4	1.21E-04	2.93	1.11E-04	3.01	1.31E-04	2.99	1.29E-04	3.01
	5	1.56E-05	2.96	1.39E-05	3.01	1.65E-05	2.99	1.61E-05	3.00
<b>Example 2</b>		$\nu = 1$		$\nu = 0.1$		$\nu = 0.01$		$\nu = 10^{-5}$	
scheme	refine	$L^2$ error	order	$L^2$ error	order	$L^2$ error	order	$L^2$ error	order
$\mathcal{P}_1$ IMEX RK2	1	1.01E-01	-	4.73E-01	-	7.21E-01	-	7.74E-01	-
	2	2.22E-02	2.18	9.32E-02	2.34	1.28E-01	2.49	1.41E-01	2.46
	3	5.34E-03	2.06	2.31E-02	2.01	2.96E-02	2.11	3.38E-02	2.06
	4	1.30E-03	2.03	5.95E-03	1.96	6.94E-03	2.09	8.28E-03	2.03
	5	3.22E-04	2.02	1.54E-03	1.96	1.67E-03	2.05	2.05E-03	2.01
$\mathcal{P}_2$ IMEX RK3	1	1.35E-02	-	5.14E-02	-	7.26E-02	-	7.89E-02	-
	2	1.61E-03	3.07	5.76E-03	3.16	9.20E-03	2.98	1.07E-02	2.88
	3	2.18E-04	2.89	7.21E-04	3.00	1.04E-03	3.15	1.47E-03	2.87
	4	2.81E-05	2.96	9.21E-05	2.97	1.17E-04	3.15	2.10E-04	2.81
	5	3.58E-06	2.98	1.17E-05	2.97	1.38E-05	3.08	3.04E-05	2.79

To verify the stability of the IMEX LDG schemes, we consider Example 1 with different  $\nu$ . Table 3 lists the maximum time step  $\tau_0$  which can be chosen to ensure the stability (in the sense that the  $L^2$ -norm of the numerical solution decreases with time) of the second and the third order IMEX LDG schemes, on both uniform rectangular and triangular meshes. In all the tests, the final computing time is  $T = 100$ , the number of elements is 6400 for rectangular mesh and 2048 for triangular mesh. From this table, we can see that the maximum time step  $\tau_0$  is approximately proportional to the diffusion coefficient  $\nu$ .

## 7 Concluding remarks

We have considered several specific implicit-explicit time marching methods coupled with the LDG schemes for solving multi-dimensional nonlinear convection-diffusion problems

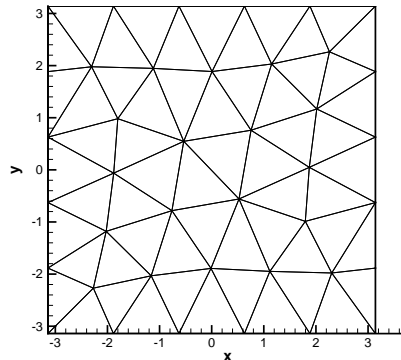


Figure 3: The initial triangular mesh.

 Table 3: The maximum time step  $\tau_0$  to ensure that the  $L^2$ -norm decreases with time for the schemes.

scheme	rectangular mesh			triangular mesh		
	$\nu = 0.1$	$\nu = 0.5$	$\nu = 1$	$\nu = 0.1$	$\nu = 0.5$	$\nu = 1$
IMEX RK2 ( $\mathcal{P}_1$ )	0.076	0.349	0.705	0.055	0.367	0.717
IMEX RK3 ( $\mathcal{P}_2$ )	0.256	1.365	2.932	0.199	1.027	1.669

with periodic boundary conditions. In multi-dimensions, the IMEX LDG schemes are unconditionally stable for the convection-diffusion problems, in the sense that the time-step  $\tau$  is only required to be upper-bounded by a positive constant independent of the spatial mesh size  $h$ . Furthermore, by the aid of the so-called elliptic projection and the adjoint argument, we obtain optimal error estimates for the corresponding fully discrete IMEX LDG schemes under the same condition as the stability analysis. Numerical examples are also given to verify our main results. Although the study in this paper is restricted to periodic boundary conditions, we expect the stability result to hold for other types of boundary conditions with a slight modification of the numerical flux at the boundary. Optimal error estimates can also be achieved for homogeneous boundary conditions, see for example [11] for such a discussion in the one-dimensional drift-diffusion models. For time dependent boundary conditions, accurate numerical boundary conditions for high order (greater than second order) IMEX-RK methods would require further investigation, which will be studied in our future work.

## 8 Appendix

In this Appendix, we would like to give the proof for Lemma 3.2. We will finish it in the following steps:

**Step 0: two projections.** First we would like to give the following two identities

which will be used several times:

$$\eta_u = U - U_h = U - PU + PU - U_h = U - PU + P\eta_u, \quad (8.1a)$$

$$\eta_q = Q - Q_h = Q - \Pi Q + \Pi Q - Q_h = Q - \Pi Q + \Pi\eta_q. \quad (8.1b)$$

where  $P$  and  $\Pi$  are the two projections defined as follows.

For both rectangular and triangular meshes in the multi-dimensional space, we use the  $L^2$  projection denoted by  $P$  for scalar-valued functions, i.e, for any  $w \in H^1(\Omega_h)$ ,

$$(w - Pw, v)_K = 0, \quad \forall v \in \mathcal{P}_k(K). \quad (8.2)$$

In this paper  $H^1(\Omega_h)$  is the broken Sobolev space

$$H^1(\Omega_h) = \{ \phi \in L^2(\Omega) : \phi|_K \in H^1(K), \forall K \in \Omega_h \}, \quad (8.3)$$

also we denote  $\mathbf{H}^1(\Omega_h) = (H^1(\Omega_h))^d$  as the broken Sobolev space in the multi-dimensional space.

For vector-valued functions on triangular elements, we will adopt the projection proposed in [5, 9], which is defined as follows: for  $\boldsymbol{\rho} \in \mathbf{H}^1(\Omega_h)$ , and an arbitrary  $K \in \Omega_h$ , given the fixed vector  $\boldsymbol{\beta}$ , and an arbitrary edge  $\tilde{e} \in \partial K$  satisfying  $\boldsymbol{\beta} \cdot \mathbf{n}_K|_{\tilde{e}} > 0$ , the restriction of  $\Pi\boldsymbol{\rho}$  on  $K$  is defined as the element of  $\mathcal{P}_k(K)$  that satisfies

$$(\Pi\boldsymbol{\rho} - \boldsymbol{\rho}, \mathbf{v})_K = 0, \quad \forall \mathbf{v} \in \mathcal{P}_{k-1}(K), \quad (8.4a)$$

$$\langle (\Pi\boldsymbol{\rho} - \boldsymbol{\rho}) \cdot \mathbf{n}_K|_e, v \rangle_e = 0, \quad \forall v \in \mathcal{P}_k(e), \forall e \subset \partial K, e \neq \tilde{e}. \quad (8.4b)$$

*Remark 8.1.* The projection (8.4) is well-defined on triangles, i.e, the projection exists and is unique; see [5] for more details. Furthermore, from the definition we can conclude that, for both type-I and type-II triangles, the projection  $\Pi$  (8.4) has the following property:

$$(\Pi\boldsymbol{\rho} - \boldsymbol{\rho}, \mathbf{v})_K = 0, \quad \forall \mathbf{v} \in \mathcal{P}_{k-1}(K), \quad (8.5a)$$

$$\langle (\Pi\boldsymbol{\rho} - \boldsymbol{\rho}) \cdot \mathbf{n}_K, v \rangle_{\partial K^-} = 0, \quad \forall v \in \mathcal{P}_k(K). \quad (8.5b)$$

For vector-valued functions on rectangular meshes, we propose a similar projection as (8.4), which is defined as follows: for  $\boldsymbol{\rho} \in \mathbf{H}^1(\Omega_h)$ , and an arbitrary  $K \in \Omega_h$ , the restriction of  $\Pi\boldsymbol{\rho}$  on  $K$  is defined as the element of  $\mathcal{P}_k(K)$  that satisfies (8.5).

The projection (8.5) on rectangular element exists uniquely. Since the dimension of the freedom matches with the unknown variables, we only need to show  $\Pi\boldsymbol{\rho} = 0$  if  $\boldsymbol{\rho} = 0$ . Same as the proof of Lemma 3.2 in [5], we can obtain this conclusion easily. Owing to the orthogonality of  $\{\mathbf{n}_i\}_{i=1}^d$ , we can express  $\Pi\boldsymbol{\rho}$  as

$$\Pi\boldsymbol{\rho} = \sum_{i=1}^d z_i \mathbf{n}_i, \quad \text{where } z_i \in \mathcal{P}_k(K).$$

It is obvious that  $\Pi\boldsymbol{\rho} \cdot \mathbf{n}_i = z_i$ , for  $i = 1, \dots, d$ . Then taking the test function as  $v = z_i|_{e_i}$  in (8.5b), we can get  $z_i = 0$  on  $e_i$ . Hence  $z_i = (x - x_i)p_i$ , for some  $p_i \in \mathcal{P}_{k-1}(K)$ . Next taking  $v = p_i \mathbf{n}_i$  in (8.5a), we get

$$(\Pi\boldsymbol{\rho}, p_i \mathbf{n}_i)_K = (z_i, p_i)_K = ((x - x_i)p_i, p_i)_K.$$

Since  $x - x_i > 0$  on  $K$  except on a zero measure set  $e_i$ , we get  $p_i \equiv 0$  on  $K$ . Hence  $z_i \equiv 0$  on  $K$ , and hence  $\Pi \boldsymbol{\rho} \equiv 0$  on  $K$ .

Along the similar analysis as in [5], we have the following approximation properties. For arbitrary  $w \in H^r(\Omega)$  and  $\boldsymbol{\rho} \in \mathbf{H}^r(\Omega)$ , by the standard scaling argument [4], we have the following approximation properties

$$|w - \mathbf{P}w|_{H^m(\Omega_h)} + h^{1/2-m} \|w - \mathbf{P}w\|_{\Gamma_h} \leq Ch^{\min\{r, k+1\}-m} \|w\|_{H^r(\Omega)}, \quad (8.6a)$$

$$|\boldsymbol{\rho} - \Pi \boldsymbol{\rho}|_{\mathbf{H}^m(\Omega_h)} + h^{1/2-m} \|(\boldsymbol{\rho} - \Pi \boldsymbol{\rho}) \cdot \mathbf{n}\|_{\Gamma_h} \leq Ch^{\min\{r, k+1\}-m} \|\boldsymbol{\rho}\|_{\mathbf{H}^r(\Omega)}, \quad (8.6b)$$

for  $0 \leq m \leq \min\{r, k+1\}$ , where the bounding constant  $C > 0$  is independent of  $h$ , and  $|\cdot|_{H^m(\Omega_h)} = (\sum_{K \in \Omega_h} |\cdot|_{H^m(K)}^2)^{1/2}$ .

**Step 1: estimate  $\eta_{\mathbf{q}}$ .** First, since  $\mathbf{Q} = \nabla U$  is continuous, we have  $(\mathbf{Q}, \mathbf{r})_{\Omega_h} = \mathcal{Q}(U, \mathbf{r})$ , for arbitrary  $\mathbf{r} \in \mathbf{V}_h$ . Hence from (3.30) we have

$$\mathcal{L}(\eta_{\mathbf{q}}, v) = 0, \quad (8.7a)$$

$$(\eta_{\mathbf{q}}, \mathbf{r})_{\Omega_h} = \mathcal{Q}(\eta_u, \mathbf{r}), \quad (8.7b)$$

for arbitrary  $(v, \mathbf{r}) \in V_h \times \mathbf{V}_h$ . That is

$$-\mathcal{L}(\Pi \eta_{\mathbf{q}}, v) = \mathcal{L}(\mathbf{Q} - \Pi \mathbf{Q}, v), \quad (8.8a)$$

$$(\Pi \eta_{\mathbf{q}}, \mathbf{r})_{\Omega_h} - \mathcal{Q}(\mathbf{P} \eta_u, \mathbf{r}) = -(\mathbf{Q} - \Pi \mathbf{Q}, \mathbf{r})_{\Omega_h} + \mathcal{Q}(U - \mathbf{P}U, \mathbf{r}). \quad (8.8b)$$

Taking  $v = \mathbf{P} \eta_u$  and  $\mathbf{r} = \Pi \eta_{\mathbf{q}}$  in (8.8), and adding them together we get

$$\|\Pi \eta_{\mathbf{q}}\|^2 = -(\mathbf{Q} - \Pi \mathbf{Q}, \Pi \eta_{\mathbf{q}})_{\Omega_h} + \mathcal{Q}(U - \mathbf{P}U, \Pi \eta_{\mathbf{q}}) + \mathcal{L}(\mathbf{Q} - \Pi \mathbf{Q}, \mathbf{P} \eta_u),$$

owing to Lemma 4.1. Recalling the definitions of  $\mathcal{Q}(\cdot, \cdot)$  and the projection  $\mathbf{P}$ , we have

$$\mathcal{Q}(U - \mathbf{P}U, \Pi \eta_{\mathbf{q}}) = \langle U - \widetilde{\mathbf{P}}U, \Pi \eta_{\mathbf{q}} \cdot \mathbf{n} \rangle_{\partial \Omega_h}. \quad (8.9)$$

Here and below

$$\langle z, \mathbf{w} \cdot \mathbf{n} \rangle_{\partial \Omega_h} = \sum_{K \in \Omega_h} \langle z, \mathbf{w} \cdot \mathbf{n}_K \rangle_{\partial K}, \quad \forall (z, \mathbf{w}) \in H^1(\Omega_h) \times \mathbf{H}^1(\Omega_h).$$

Similarly, we can derive

$$\mathcal{L}(\mathbf{Q} - \Pi \mathbf{Q}, \mathbf{P} \eta_u) = - \sum_{K \in \Omega_h} \langle (\mathbf{Q} - \widetilde{\Pi \mathbf{Q}}) \cdot \mathbf{n}_K, \llbracket \mathbf{P} \eta_u \rrbracket \rangle_{\partial K^-} = 0, \quad (8.10)$$

by the property of  $\Pi$  (8.5) and the choice of the numerical flux  $\widetilde{\Pi \mathbf{Q}} = (\Pi \mathbf{Q})^+$ . Hence, by the Cauchy-Schwarz inequality, the inverse inequality (3.1), and the approximation property (8.6) we get

$$\|\Pi \eta_{\mathbf{q}}\|^2 \leq \left[ \|\mathbf{Q} - \Pi \mathbf{Q}\| + h^{-1/2} \|U - \mathbf{P}U\|_{\Gamma_h} \right] \|\Pi \eta_{\mathbf{q}}\| \leq Ch^k \|\Pi \eta_{\mathbf{q}}\|,$$

which yields the result

$$\|\eta_{\mathbf{q}}\| + h^{1/2} \|\eta_{\mathbf{q}} \cdot \mathbf{n}\|_{\Gamma_h} \leq Ch^k, \quad (8.11)$$

by using the triangle inequality, the inverse inequality (3.1) and the approximation property (8.6).

**Step 2: estimate  $\eta_u$ .** To this end, we need the following lemma, whose proof will be postponed to Step 3.

**Lemma 8.1.** *For arbitrary  $\zeta$  we have*

$$\begin{aligned} (\mathbf{P}\eta_u, \zeta)_{\Omega_h} &= \langle U - \widetilde{\mathbf{P}}U, (\Pi\boldsymbol{\psi} - \boldsymbol{\psi}) \cdot \mathbf{n} \rangle_{\partial\Omega_h} + (\eta_{\mathbf{q}}, \boldsymbol{\psi} - \Pi\boldsymbol{\psi})_{\Omega_h} \\ &\quad - (\mathbf{P}\varphi - \varphi, \nabla \cdot (\mathbf{Q} - \Pi\mathbf{Q}))_{\Omega_h} + \langle (\eta_{\mathbf{q}} - \tilde{\eta}_{\mathbf{q}}) \cdot \mathbf{n}, \mathbf{P}\varphi - \varphi \rangle_{\partial\Omega_h}, \end{aligned} \quad (8.12)$$

where  $\zeta$  is the term on the right-hand side of the adjoint elliptic problem (3.33).

Now we continue our proof of the second step. By taking  $\zeta = \mathbf{P}\eta_u$  in (8.12), and by the Cauchy-Schwarz inequality we get

$$\begin{aligned} \|\mathbf{P}\eta_u\|^2 &\leq \|\mathbf{P}U - U\|_{\Gamma_h} \|(\boldsymbol{\psi} - \Pi\boldsymbol{\psi}) \cdot \mathbf{n}\|_{\Gamma_h} + \|\eta_{\mathbf{q}}\| \|\boldsymbol{\psi} - \Pi\boldsymbol{\psi}\| \\ &\quad + \|\mathbf{Q} - \Pi\mathbf{Q}\|_{H^1} \|\varphi - \mathbf{P}\varphi\| + \|\eta_{\mathbf{q}} \cdot \mathbf{n}\|_{\Gamma_h} \|\mathbf{P}\varphi - \varphi\|_{\Gamma_h}. \end{aligned}$$

Hence, it follows from (8.11) and (8.6) that

$$\begin{aligned} \|\mathbf{P}\eta_u\|^2 &\leq Ch^{k+\min\{1, k+1\}} \|\boldsymbol{\psi}\|_{H^1} + Ch^{k+\min\{2, k+1\}} \|\varphi\|_{H^2} + Ch^{k-1+\min\{2, k+1\}} \|\varphi\|_{H^2} \\ &\leq Ch^{k+1} (\|\boldsymbol{\psi}\|_{H^1} + \|\varphi\|_{H^2}) \leq C C_* h^{k+1} \|\mathbf{P}\eta_u\|, \end{aligned} \quad (8.13)$$

if  $k \geq 1$ , where  $C$  only depends on the regularity of  $U$ , and the last inequality holds by the elliptic regularity assumption (3.34). Hence we obtain

$$\|\mathbf{P}\eta_u\| \leq Ch^{k+1}, \quad (8.14)$$

which implies the result of Lemma 3.2.

**Step 3: proof of Lemma 8.1.** By (3.33) we have

$$(\mathbf{P}\eta_u, \zeta)_{\Omega_h} = (\mathbf{P}\eta_u, \nabla \cdot \boldsymbol{\psi})_{\Omega_h} = (\nabla \cdot \boldsymbol{\psi}, \mathbf{P}\eta_u)_{\Omega_h} = \mathcal{L}(\boldsymbol{\psi}, \mathbf{P}\eta_u),$$

since  $\boldsymbol{\psi}$  is continuous. Hence by the similar argument as (8.10) and by Lemma 4.1 we get

$$\begin{aligned} (\mathbf{P}\eta_u, \zeta)_{\Omega_h} &= \mathcal{L}(\boldsymbol{\psi} - \Pi\boldsymbol{\psi}, \mathbf{P}\eta_u) + \mathcal{L}(\Pi\boldsymbol{\psi}, \mathbf{P}\eta_u) = -\mathcal{Q}(\mathbf{P}\eta_u, \Pi\boldsymbol{\psi}) \\ &= \mathcal{Q}(U - \mathbf{P}U, \Pi\boldsymbol{\psi}) - \mathcal{Q}(\eta_u, \Pi\boldsymbol{\psi}). \end{aligned}$$

As a result, similar as (8.9) and by (8.7b) we have

$$\begin{aligned} (\mathbf{P}\eta_u, \zeta)_{\Omega_h} &= \langle U - \widetilde{\mathbf{P}}U, \Pi\boldsymbol{\psi} \cdot \mathbf{n} \rangle_{\partial\Omega_h} - (\eta_{\mathbf{q}}, \Pi\boldsymbol{\psi}) \\ &= \langle U - \widetilde{\mathbf{P}}U, (\Pi\boldsymbol{\psi} - \boldsymbol{\psi}) \cdot \mathbf{n} \rangle_{\partial\Omega_h} - (\eta_{\mathbf{q}}, \Pi\boldsymbol{\psi}), \end{aligned} \quad (8.15)$$

where we have used the fact  $\langle U - \widetilde{\mathbf{P}}U, \boldsymbol{\psi} \cdot \mathbf{n} \rangle_{\partial\Omega_h} = 0$ , since both  $U$  and  $\boldsymbol{\psi}$  are continuous across the element interface.

Denote  $A_1 = -(\eta_{\mathbf{q}}, \Pi\psi)_{\Omega_h}$ . From (3.33) we have

$$A_1 = (\eta_{\mathbf{q}}, \psi - \Pi\psi)_{\Omega_h} - (\eta_{\mathbf{q}}, \psi)_{\Omega_h} = (\eta_{\mathbf{q}}, \psi - \Pi\psi)_{\Omega_h} - (\eta_{\mathbf{q}}, \nabla\varphi)_{\Omega_h}. \quad (8.16)$$

Denote  $A_2 = -(\eta_{\mathbf{q}}, \nabla\varphi)_{\Omega_h}$ , we can derive that

$$\begin{aligned} A_2 &= (\eta_{\mathbf{q}}, \nabla(\mathbf{P}\varphi - \varphi))_{\Omega_h} - (\eta_{\mathbf{q}}, \nabla\mathbf{P}\varphi)_{\Omega_h} \\ &= -(\mathbf{P}\varphi - \varphi, \nabla \cdot \eta_{\mathbf{q}})_{\Omega_h} + \langle \eta_{\mathbf{q}} \cdot \mathbf{n}, \mathbf{P}\varphi - \varphi \rangle_{\partial\Omega_h} - \langle \tilde{\eta}_{\mathbf{q}} \cdot \mathbf{n}, \mathbf{P}\varphi \rangle_{\partial\Omega_h}, \end{aligned}$$

where the second identity is obtained through integrating by parts and (8.7a).

Since both  $\mathbf{Q}$  and  $\phi$  are continuous across the element interface, we can verify that

$$\langle \tilde{\eta}_{\mathbf{q}} \cdot \mathbf{n}, \varphi \rangle_{\partial\Omega_h} = 0.$$

Then by the property of the projection  $\mathbf{P}$  we have

$$\begin{aligned} A_2 &= -(\mathbf{P}\varphi - \varphi, \nabla \cdot (\eta_{\mathbf{q}} - \Pi\eta_{\mathbf{q}}))_{\Omega_h} + \langle (\eta_{\mathbf{q}} - \tilde{\eta}_{\mathbf{q}}) \cdot \mathbf{n}, \mathbf{P}\varphi - \varphi \rangle_{\partial\Omega_h} \\ &= -(\mathbf{P}\varphi - \varphi, \nabla \cdot (\mathbf{Q} - \Pi\mathbf{Q}))_{\Omega_h} + \langle (\eta_{\mathbf{q}} - \tilde{\eta}_{\mathbf{q}}) \cdot \mathbf{n}, \mathbf{P}\varphi - \varphi \rangle_{\partial\Omega_h}. \end{aligned} \quad (8.17)$$

Consequently, combining (8.15), (8.16) and (8.17) we can obtain (8.12).  $\square$

## References

- [1] U. M. ASCHER, S. J. RUUTH AND R. J. SPITERI, *Implicit-explicit Runge-Kutta methods for time-dependent partial differential equations*, Appl. Numer. Math., 25 (1997), pp. 151–167.
- [2] F. BASSI AND S. REBAY, *A high-order accurate discontinuous finite element method for the numerical solution of the compressible Navier-Stokes equations*, J. Comput. Phys., 131 (1997), pp. 267–279.
- [3] M. P. CALVO, J. DE FRUTOS AND J. NOVO, *Linearly implicit Runge-Kutta methods for advection-reaction-diffusion equations*, Appl. Numer. Math., 37 (2001), pp. 535–549.
- [4] P. G. CIARLET, *The Finite Element Method for Elliptic Problems*, North-Holland, Amsterdam, New York, 1978.
- [5] B. COCKBURN AND B. DONG, *An analysis of the minimal dissipation local discontinuous Galerkin method for convection-diffusion problems*, J. Sci. Comput., 32 (2007), pp. 233–262.
- [6] B. COCKBURN, G. KANSCHAT, I. PERUGIA AND D. SCHÖTZAU, *Superconvergence of the local discontinuous Galerkin method for elliptic problems on rectangular grids*, SIAM J. Numer. Anal., 39 (2001), pp. 264–285.
- [7] B. COCKBURN AND C.-W. SHU, *The local discontinuous Galerkin method for time-dependent convection-diffusion systems*, SIAM J. Numer. Anal., 35 (1998), pp. 2440–2463.

- [8] B. COCKBURN AND C.-W. SHU, *Runge-Kutta discontinuous Galerkin methods for convection-dominated problems*, J. Sci. Comput., 16 (2001), pp. 173–261.
- [9] B. DONG AND C.-W. SHU, *Analysis of a local discontinuous Galerkin methods for linear time-dependent fourth-order problems*, SIAM J. Numer. Anal., 47 (2009), pp. 3240–3268.
- [10] R. S. FALK AND G. R. RICHTER, *Analysis of a continuous finite element method for hyperbolic equations*, SIAM J. Numer. Anal., 24 (1987), pp. 257–278.
- [11] Y. LIU AND C.-W. SHU, *Analysis of the local discontinuous Galerkin method for the drift-diffusion model of semiconductor devices*, Sci. China Math., to appear. doi: 10.1007/s11425-015-5055-8
- [12] C.-W. SHU, *Discontinuous Galerkin methods: general approach and stability*, Numerical Solutions of Partial Differential Equations, S. Bertoluzza, S. Falletta, G. Russo and C.-W. Shu, Advanced Courses in Mathematics CRM Barcelona, Birkhauser, Basel, 2009, pp. 149–201.
- [13] V. THOMÉ, *Galerkin finite element methods for parabolic problems*, 2nd ed., Springer Ser. Comput. Math., Springer-Verlag, Berlin, 2007.
- [14] H. J. WANG, C.-W. SHU AND Q. ZHANG, *Stability and error estimates of the local discontinuous Galerkin method with implicit-explicit time-marching for advection-diffusion problems*, SIAM J. Numer. Anal., 53 (2015), pp. 206–227.
- [15] H. J. WANG, C.-W. SHU AND Q. ZHANG, *Stability and error estimates of the local discontinuous Galerkin method with implicit-explicit time-marching for nonlinear convection-diffusion problems*, Appl. Math. Comput. (2015), <http://dx.doi.org/10.1016/j.amc.2015.02.067>
- [16] H. J. WANG AND Q. ZHANG, *Error estimate on a fully discrete local discontinuous Galerkin method for linear convection-diffusion problem*, J. Comput. Math., 31 (2013), pp. 283–307.
- [17] M. F. WHEELER, *A priori  $L_2$  error estimates for Galerkin approximations to parabolic partial differential equations*, SIAM J. Numer. Anal., 10 (1973), pp. 723–759.
- [18] Y. H. XIA, Y. XU AND C.-W. SHU, *Efficient time discretization for local discontinuous Galerkin methods*, Discrete Contin. Dyn. Syst. Ser. B, 8 (2007), pp. 677–693.
- [19] Y. H. XIA, Y. XU AND C.-W. SHU, *Application of the local discontinuous Galerkin method for the Allen-Cahn/Cahn-Hilliard system*, Commun. Comput. Phys., 5 (2009), pp. 821–835.
- [20] Y. XU AND C.-W. SHU, *Local discontinuous Galerkin methods for the Kuramoto-Sivashinsky equations and the Ito-type coupled KdV equations*. Comput. Methods Appl. Mech. Engrg., 195 (2006), pp. 3430–3447.

- [21] Y. XU AND C.-W. SHU, *Local discontinuous Galerkin methods for high-order time-dependent partial differential equations*, Commun. Comput. Phys., 7 (2010), pp. 1–46.
- [22] J. YAN AND C.-W. SHU, *A local discontinuous Galerkin method for KdV type equations*, SIAM J. Numer. Anal., 40 (2002), pp. 769–791.
- [23] J. YAN AND C.-W. SHU, *Local discontinuous Galerkin methods for partial differential equations with higher order derivatives*, J. Sci. Comput., 17 (2002), pp. 17–27.
- [24] Q. ZHANG AND C.-W. SHU, *Error estimates to smooth solution of Runge-Kutta discontinuous Galerkin methods for scalar conservation laws*, SIAM J. Numer. Anal., 42 (2004), pp. 641–666.
- [25] Q. ZHANG AND C.-W. SHU, *Stability analysis and a priori error estimates to the third order explicit Runge-Kutta discontinuous Galerkin method for scalar conservation laws*, SIAM J. Numer. Anal., 48 (2010), pp. 1038–1063.